

# THE ROLE OF MICRORNA-26A IN SKELETAL MUSCLE INSULIN SIGNALING

by

Jonathan Joseph Petrocelli

A thesis submitted to the faculty of  
the University of North Carolina at Charlotte  
in partial fulfillment of the requirements  
for the degree of Master of Science in  
Kinesiology

Charlotte

2018

Approved by:

---

Dr. Joseph Marino

---

Dr. Susan Arthur

---

Dr. Kirill Afonin

---

Dr. Michael Turner

©2018  
Jonathan Joseph Petrocelli  
ALL RIGHTS RESERVED

## ABSTRACT

JONATHAN JOSEPH PETROCELLI. The role of microRNA-26a in skeletal muscle insulin signaling. (Under the direction of DR. JOSEPH S. MARINO).

Chronic saturated fatty acid exposure causes skeletal muscle cells to develop insulin resistance, which contributes to the pathogenesis of type 2 diabetes mellitus. Recently, microRNAs have been viewed as novel molecules that contribute to the regulation of insulin responsiveness when cells are challenged with fatty acids. The aim of the present study was to identify the role of miR-26a in skeletal muscle cells insulted with a chronic exposure of palmitic acid (PA). A C2C12 cell culture model was utilized and protein and RNA expression was evaluated using Western blot analysis and real time polymerase chain reaction, respectively. The results of our study indicate that PA reduces insulin responsiveness in myoblasts through reductions in total and phosphorylated protein kinase B (AKT). Reduced phosphorylated AKT is suggestive of diminished glucose uptake ability and other insulin-sensitive processes. Additionally, we observed that overexpressing miR-26a was not able to alleviate the decreased signaling caused by chronic PA treatment. In conclusion, our study identified that miR-26a may not have a central role in regulating PA-induced insulin resistance in myoblasts. However, the impaired insulin response in myoblasts observed in our study eludes to a disruption in the myogenic program through AKT, which may have negative implications in muscle growth and regeneration, as well as contributing to glucose intolerance.

## TABLE OF CONTENTS

LIST OF FIGURES	vi
LIST OF ABBREVIATIONS	vii
CHAPTER 1: INTRODUCTION	1
CHAPTER 2: LITERATURE REVIEW	4
2.1 Regulation of Skeletal Muscle Insulin Signaling	4
2.2 Insulin Signaling in the Myogenic Program	8
2.3 Introduction to microRNAs	9
2.4 miRNA Biogenesis and Function	10
2.5 miRNA Skeletal Muscle Profiling in Type 2 Diabetes	12
2.6 miRNAs Affecting the Insulin Signaling Pathway	12
2.7 The Effect of miR-26a on Insulin Signaling	15
2.8 Regulation of miR-26a	16
2.9 Conclusion	17
CHAPTER 3: METHODS	19
3.1 Cell Culture and Treatment	19
3.2 Palmitic Acid Solution	19
3.3 Experimental Design	19
3.4 Western Blot Analysis	21
3.5 RNA Isolation and RT-qPCR	21
3.6 Bioinformatics Predictions	22
3.7 miR-26a Dose Response	22

3.8	Flow Cytometry	23
3.9	Puromycin Incorporation	23
3.10	Statistical Analysis	24
CHAPTER 4: RESULTS		25
4.1	The Effect of PA Exposure on Insulin Responsiveness	25
4.2	Palmitic Acid Treatment Decreases Endogenous levels of miR-26a	27
4.3	Optimizing miR-26a Mimic in C2C12 Myoblasts	27
4.4	miR-26a Overexpression Does Not Alter AKT Phosphorylation Status in Cells Treated with Palmitic Acid	28
4.5	Palmitic Acid Decreases Endogenous Levels of PTEN in Myoblasts	29
4.6	Palmitic Acid Does Not Increase Muscle Protein Breakdown	31
CHAPTER 5: DISCUSSION		33
CHAPTER 6: CONCLUSION		37
REFERENCES		38
APPENDIX: ORIGINAL WESTERN BLOTS USED FOR ANALYSIS		44

## LIST OF FIGURES

FIGURE 1: Homeostatic skeletal muscle insulin signaling.	4
FIGURE 2: PTEN and PKC $\theta$ effects on the insulin signaling pathway in skeletal muscle.	7
FIGURE 3: MicroRNA biogenesis pathway.	10
FIGURE 4: Proposed miR-26a regulation in skeletal muscle insulin signaling when challenged with free fatty acids.	17
FIGURE 5: Experimental design.	20
FIGURE 6: Optimization of miR-26a mimic and transfection reagent dose.	23
FIGURE 7: The effect of palmitic acid exposure on insulin responsiveness.	25–26
FIGURE 8: Palmitic acid treatment decreases endogenous levels of miR-26a.	27
FIGURE 9: Optimization of miR-26a mimic.	29
FIGURE 10: miR-26a overexpression does not alter AKT phosphorylation status in cells treated with palmitic acid.	30
FIGURE 11: Palmitic acid decreases endogenous levels of PTEN.	31
FIGURE 12: Muscle protein breakdown measured by puromycin incorporation.	32
FIGURE 13: Proposed mechanism of palmitic acid effects on skeletal muscle cells.	35

## LIST OF ABBREVIATIONS

AKT	protein kinase B
ANOVA	analysis of variance
C/EBP $\alpha$	CCAAT/enhancer-binding protein alpha
cDNA	complimentary DNA
CTDSPL	CTD small phosphatase-like protein
DAG	diacylglycerol
DGCR8	DiGeorge syndrome chromosomal region 8
DMEM	Dulbecco's modified eagle's medium
FAF-BSA	fatty acid free bovine serum albumin
FBS	fetal bovine serum
GLUT4	glucose transporter type 4
GSK3 $\beta$	glycogen synthase kinase 3 beta
INSR	insulin receptor
IRS-1	insulin receptor substrate-1
IRS-2	insulin receptor substrate-2
kDa	Kilodalton
m <sup>7</sup> G	7-methyl-guanosine cap
miRNA	microRNA
mRNA	messenger RNA
mTOR	mechanistic target of rapamycin
mTOR2C	mechanistic target of rapamycin complex 2
PA	palmitic acid
PDK1	pyruvate dehydrogenase lipoamide kinase isozyme 1

PI3K	phosphoinositide 3-kinase
PIP <sub>3</sub>	phosphatidylinositol (3,4,5)-trisphosphate
PKC $\delta$	protein kinase C delta
PKC $\theta$	protein kinase C theta
pre-miRNA	precursor microRNA
pri-miRNA	primary microRNA
PTEN	phosphatase and tensin homolog
RISC	RNA induced silencing complex
SH2	src homology 2
T2DM	type 2 diabetes mellitus
TBS	tris buffered saline
TBS-T	tris buffered saline-tween
TFR	transfection reagent
TRBP	TAR RNA binding protein

## CHAPTER 1: INTRODUCTION

Type 2 diabetes mellitus (T2DM) is a metabolic disease which as of 2014 affects roughly 400 million people globally [1]. T2DM is characterized by impaired insulin secretion, elevated hepatic glucose production, and insulin resistance in skeletal muscle, liver, and adipocytes [2]. Another characteristic of T2DM is elevated levels of intramyocellular lipids [3, 4]. The consumption of high fat diets causes the accumulation of intracellular lipids that results in skeletal muscle insulin resistance leading to development of hyperglycemia [5-7]. Additionally, lipid accumulation, insulin resistance, and T2DM contribute to decreased skeletal muscle regrowth and regeneration contributing to glucose dysregulation and other co-morbidities [8]. With skeletal muscle being the largest insulin responsive tissue in the body, and a primary regulator of insulin and glucose homeostasis [2, 9], a better understanding of the mechanisms unpinning insulin resistance in this tissue is critical in the development of treatment.

In skeletal muscle the breakdown of triglycerides to lipid intermediates, specifically diacylglycerol (DAG), increases the activity of protein kinases and phosphatases that inhibit insulin signaling [10-12]. With this activation, skeletal muscle insulin resistance occurs through upstream signal transduction interference, diminishing activation of glucose transporters [13]. When insulin signaling is impaired the result is reduced glucose diffusion into the cell through cytoplasmic glucose transporters, resulting in hyperglycemia [6]. If left uncontrolled, T2DM can develop along with other metabolic related disorders.

The development of lipid induced insulin resistance in skeletal muscle is a topic of current interest particularly, insulin resistance in skeletal muscle myoblasts. Myoblasts

are used *in vitro* to examine muscle cell growth and injury repair, and are highly responsive to insulin [14]. Briefly, myoblasts proliferate until reaching cell to cell contact, setting off gene regulatory factors that commit them to the myogenic program. This results in the differentiation and fusion of myoblasts into multinucleated mature muscle cells. Over time these mature cells will form muscle fibers with characteristic contractile properties [15]. Studying myoblast insulin response when cells are challenged with saturated fatty acids may provide insights into myogenic dysregulation, contributing to impaired muscle regeneration and glucose intolerance typical of T2DM patients.

Recently, lipid-induced insulin resistance in skeletal muscle has been shown to be regulated by microRNAs (miRNAs) [16]. miRNAs are a class of small non-protein coding RNAs responsible for regulating protein translation by repressing messenger RNAs (mRNAs) through binding of complementary sites on their 3'-untranslated regions (UTR) [17]. miRNAs are endogenously produced and processed, and inhibit mRNA through mRNA degradation or repressing ribosome translation [18]. Numerous miRNAs such as miR-194 [19], miR-106b [20], and miR-128a [21] have been shown to regulate insulin signaling in C2C12 mouse muscle cells. Because one miRNA could modulate responses of many different mRNAs, and each mRNA may be modulated by multiple miRNAs, further work is warranted to more completely understand the role of miRNAs in the regulation of insulin responsiveness.

miR-26a is a prime example of a miRNA that has a potential integrated role in regulating the insulin response. In liver tissue it has been found that miR-26a targets insulin signaling genes as well as genes that regulate fatty acid metabolism [22]. miR-26a overexpression was able to preserve insulin signaling, body weight, and glucose tolerance

in mice fed a high fat diet [22]. The dual role of miR-26a in balancing the metabolism of lipids with the preservation of insulin signaling make it an attractive target to explore its role in skeletal muscle that is challenged with saturated fatty acids. The purpose of our study was to determine if miR-26a can preserve insulin responsiveness in myoblasts treated with the saturated fatty acid, palmitic acid (PA). We hypothesized that miR-26a would improve insulin responsiveness when myoblasts were challenged with PA treatment.

## CHAPTER 2: LITERATURE REVIEW

### 2.1. Regulation of Skeletal Muscle Insulin Signaling

Homeostatic signal transduction through the insulin signaling pathway begins with the binding of insulin to the insulin receptor (figure 1).

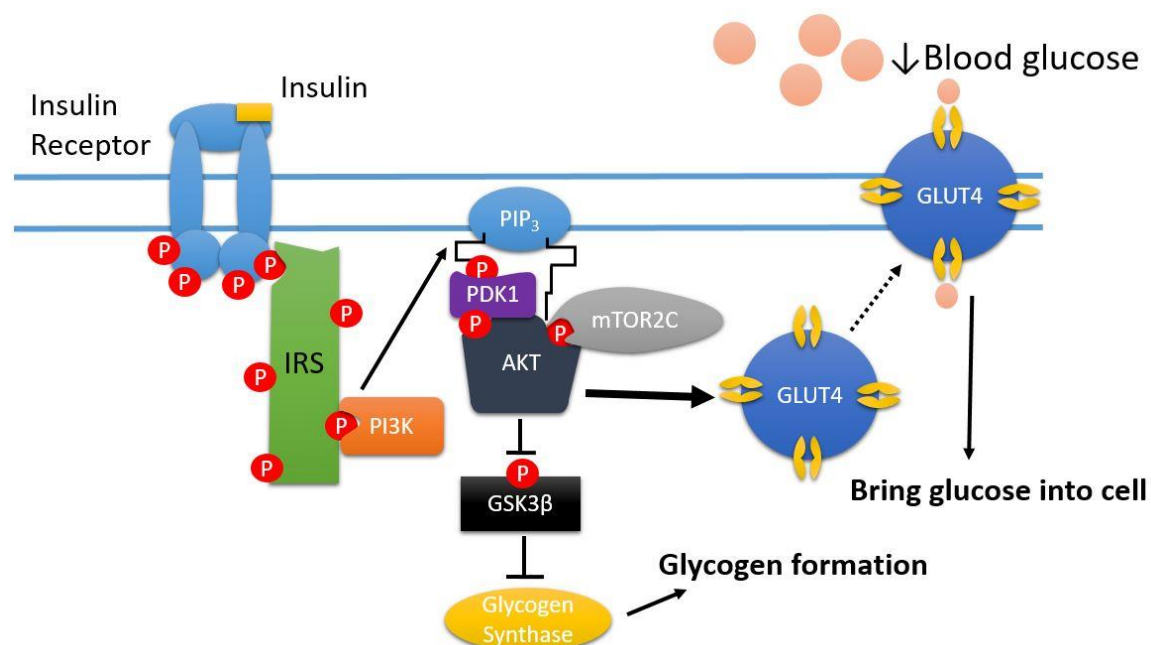


**Figure 1.** Homeostatic skeletal muscle insulin signaling. Details of signaling are provided in the text.

The insulin receptor consists of an exclusively extracellular  $\alpha$  subunit and a transmembrane  $\beta$  subunit, which are linked by disulfide bonds [23, 24]. Upon insulin binding to the  $\alpha$  subunit of the receptor, a conformational change in the  $\beta$  subunit occurs, bringing the intracellular domains into contact with each other. This conformational change exposes cytosolic tyrosine phosphorylation sites that allow the binding of substrates such as insulin receptor substrate-1 (IRS-1) [25]. This represents the first step in the action of skeletal muscle insulin signaling and glucose metabolism. In regards to

insulin resistance, the insulin receptor is not identified as a primary factor influential in pathogenesis and mutations occur only in rare cases [26].

The IRS-1 protein has multiple tyrosine residues that allow for binding of different protein domains, allowing for divergence of the pathway. With increased intramyocellular lipids, IRS-1 activity is decreased. This is primarily through protein kinase C  $\theta$  (PKC $\theta$ ) phosphorylation (figure 2A). PKC $\theta$  is activated when diacylglycerol (DAG) accumulates in the plasma membrane [27, 28]. Long-chain acyl co-enzyme A increases membrane DAG content, that subsequently leads to PKC $\theta$  activation [13]. Activation of PKC $\theta$  causes phosphorylation of IRS-1 at serine 1101 leading to decreased IRS-1 activity [11].

In homeostatic insulin signaling, after IRS-1 is activated phosphoinositide 3-kinase (PI3K) binds to the phosphorylated tyrosines on IRS-1 [29, 30]. PI3K is composed of two subunits, one containing two src homology 2 (SH2) domains and the other containing a catalytic domain. PI3K is activated directly as a consequence of binding of its two SH2 domains to tyrosine phosphorylation sites [25]. The activation of PI3K leads to the formation of membrane bound phosphoinositides, including phosphoinositide 3,4,5-triphosphate (PIP<sub>3</sub>). PIP<sub>3</sub> interacts with protein kinase B (AKT) at the plasma membrane via a PH domain. Phosphorylation of pyruvate dehydrogenase lipoamide kinase isozyme 1 (PDK1) through PIP<sub>3</sub> causes AKT to become a substrate for PDK1. PDK1 is also bound to PIP<sub>3</sub> at the membrane through a PH domain.

In instances of increased saturated fatty acids, phosphatase and tensin homolog (PTEN) acts to dephosphorylate PIP<sub>3</sub> (figure 2B). Reducing PIP<sub>3</sub> phosphorylation moderates activation of AKT resulting in reduced responsiveness to insulin. PTEN

protein and mRNA levels are increased in skeletal muscle of obese Zucker rats and Zucker rats fed a high fructose diet [31]. These rats have diminished tolerance to insulin and glucose indicating metabolic deficiencies similar to those seen in the early stages of T2DM [31]. Additionally, skeletal muscle specific deletion of the PTEN gene in mice resulted in protection against insulin resistance and T2DM development only in mice given a high fat diet [32]. This mechanism was partially caused by increased phosphorylation of AKT with PTEN deletion [32]. The direct mechanism of how PTEN increases with augmented intramyocellular lipid levels is not known. However, it may be potentially caused by a cascade involving peroxisome proliferator-activated receptor gamma, and peroxisome proliferator-activated receptor-gamma coactivator 1alpha [33, 34].

Once PDK1 and the mechanistic target of rapamycin complex 2 (mTORC2) phosphorylate AKT at threonine residue 308 and serine residue 473 respectively, AKT becomes activated and dissociates from the plasma membrane and moves into the cytosol and the cell nucleus [25]. AKT plays a major role in a number of separate signaling pathways that mediate insulin response. These pathways include the synthesis of new proteins, synthesis of glycogen, and the translocation of glucose transporters to the plasma membrane (figure 1). AKT increases glycogen synthesis through the phosphorylation of glycogen synthase 3 kinase  $\beta$  (GSK3 $\beta$ ). Glycogen synthase is the major protein responsible for the synthesis of glycogen in skeletal muscle, and is inhibited by GSK3 $\beta$ . Phosphorylation of GSK3 $\beta$  decreases its activity leading to increased glycogen formation [25].

Another major function of AKT is the translocation of the cytoplasmic glucose

transporter, glucose transporter type 4 (GLUT4). GLUT4 facilitates diffusion of glucose by translocating from the cytosol to the plasma membrane where it fuses with the plasma membrane [35]. This fusion allows for transport vesicles to become exposed to extracellular glucose and for the facilitated diffusion of glucose into skeletal muscle cells.

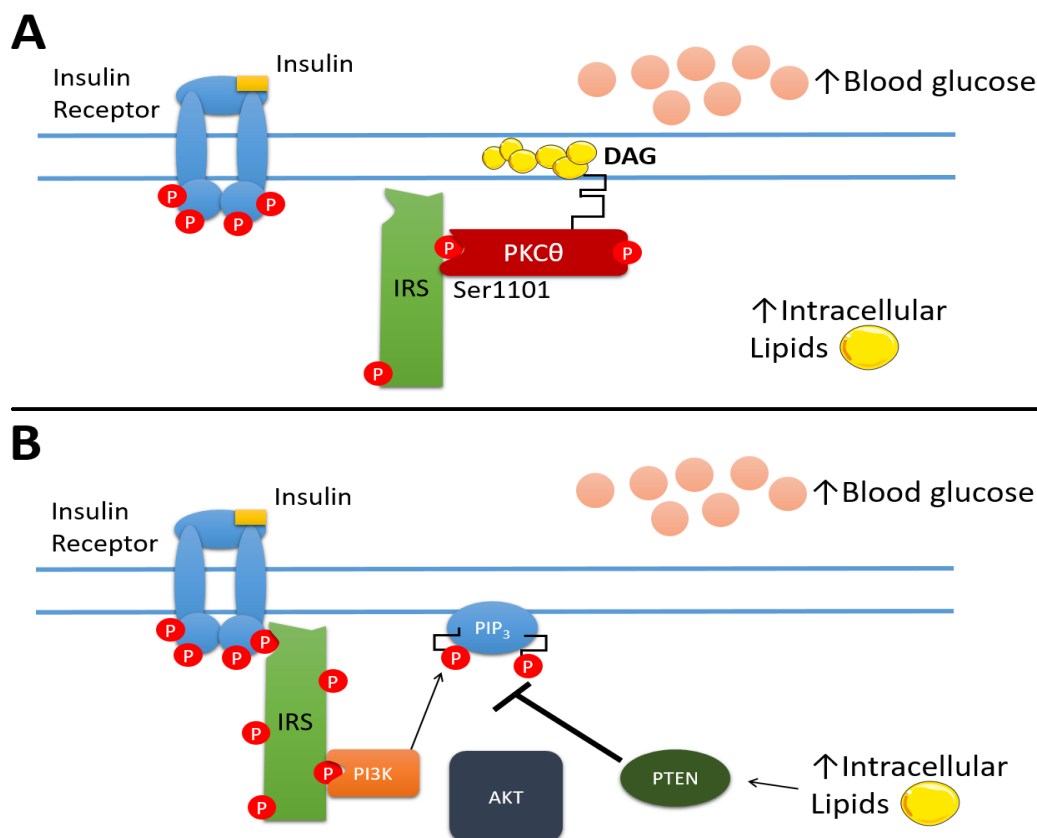


**Figure 2.** PTEN and PKCθ effects on the insulin signaling pathway in skeletal muscle. (A) Increased intramyocellular lipids expands DAG available in the plasma membrane. This recruits and activates PKCθ, resulting in phosphorylation of IRS-1 at ser1101. (B) Increased intramyocellular lipids increases PTEN expression. PTEN inhibits PIP<sub>3</sub> activation thus leading to decreased phosphorylation of AKT. Both of these actions lead to reduced phosphorylation of AKT that ultimately leads to reductions in glucose uptake, and thus amplified circulating blood glucose levels.

## **2.2. Insulin Signaling in the Myogenic Program**

Skeletal muscle development, or myogenesis, occurs with pluripotent muscle stem cells known as satellite cells. Satellite cells give rise to myoblasts, which are the precursors of contractile muscle cells [36]. Myoblasts proliferate and upon repeated cell surface contact, fuse together and differentiate to form myotubes [36]. Under the direction of differentially expressed myogenic regulatory factors, myogenesis ensues and muscle is formed.

Myoblasts are highly sensitive to insulin and express the insulin receptor in abundance [37]. Insulin action on myoblasts induces myogenesis through PI3K signaling that activates AKT [38]. Insulin has been shown to promote myoblast cycling causing proliferation [37]. Additionally, AKT activation through insulin signaling rescues myoblasts from apoptosis [37]. Insulin also plays a role in the later stages of myogenesis by promoting differentiation of myoblasts into myotubes furthering the maturation of skeletal muscle cells [38].

Intramyocellular lipid accumulation is correlated with fat mass percentage and contributes to impairments in skeletal muscle plasticity, which is controlled through myogenesis [8, 39]. The insulin resistance that ensues from lipid accumulation in muscle may contribute to decreased muscle regenerative capacity through impaired insulin signaling. Insulin-stimulated PI3K/AKT signaling is needed for myoblast proliferation and differentiation. With inhibition of this pathway, myoblast activity cannot proceed. This leads to muscle regrowth inhibition contributing to decreases in muscle mass, resulting in less glucose uptake capacity [8]. However, the exact mechanisms controlling PA impairments in myoblast insulin signaling are still under investigation.

Muscle fiber damage either through exercise or activities of daily living is a common occurrence, and is beneficial to muscle growth through regeneration processes [40]. The muscle environment is critical to regeneration and circulating fatty acids contribute to the complex dysregulation of this microenvironment. Briefly, circulating lipids result in lipid accumulation in muscle and adipocytes that enhance inflammatory responses. This leads to muscle fibrosis and impaired insulin signaling that fuels insulin resistance [39]. Myoblast insulin responsiveness may contribute towards this phenotype and investigating miRNAs may provide novel pharmacological interventions to alleviating negative muscle growth and regeneration, and glucose intolerance.

### **2.3. Introduction to MicroRNAs**

MicroRNAs (miRNAs) are a class of small, non-protein coding RNAs which play a role in regulating translation of complementary messenger RNAs (mRNA) [17, 41]. miRNAs were first discovered during studies of genes that control the timing of larval development in the worm, *Caenorhabditis elegans* [42]. Characterization of genes in these studies revealed small regulatory RNAs about 22 nucleotides long that have now been found in all metazoan studies thus far [43, 44]. There have been roughly 1,800 precursors and more than 2,500 mature miRNA sequences discovered for the human species as of 2015, and that number is likely to increase [41]. miRNAs play an important role in biological processes associated with diverse cellular activity, and are implicated in a variety of human diseases and disorders. For this reason, miRNAs are emerging as potential drug targets for gene therapy in genetic disorders, and are promising biomarkers for diseases [45, 46].

## 2.4. miRNA Biogenesis and Function

Mature miRNAs are a class of single-stranded, short (~19-24 nucleotides), evolutionally conserved, and non-protein coding RNAs. They act as post-transcriptional

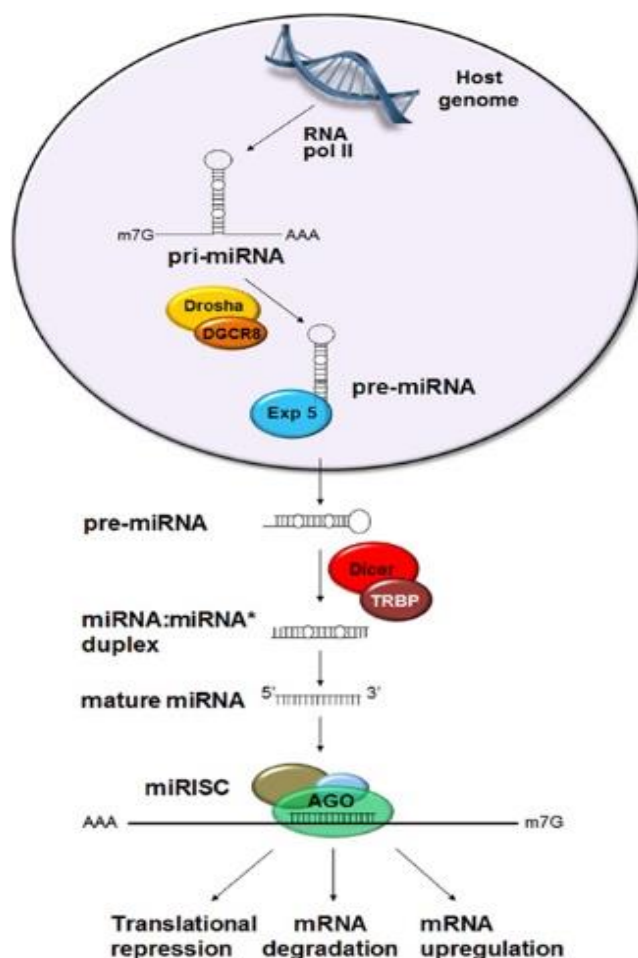


**Figure 3.** MicroRNA biogenesis pathway. Details are described in the text. DiGeorge syndrome chromosomal region 8 (DGCR8) is the vertebrate equivalent to Pasha. TAR RNA binding protein (TRBP) aids in Dicer cleavage of miRNA duplex. Figure derived from [47].

negative regulators of gene expression by binding to mRNAs [41]. miRNA-mediated gene repression begins with the generation of a primary transcript (figure 3), also termed the primary microRNA (pri-miRNA) [45]. miRNAs are initially transcribed by RNA polymerase II with some miRNAs being used by RNA polymerase III to generate the long pri-RNAs with one or more hairpin structures in the cell nucleus. The pri-miRNA is recognized and cleaved in the nucleus by the enzyme Drosha, and a RNA-binding protein Pasha, in order to generate a 70-100 nucleotide precursor microRNA (pre-miRNA) with a stem-loop

structure. The pre-miRNA is then translocated into the cytoplasm by the nuclear receptor Exportin-5 and Ran-GTP, where it is further processed into a 19-24 nucleotide miRNA

duplex by the enzyme Dicer. The dissociation of the duplex gives rise to a mature miRNA molecule incorporated into an Argonaute protein, forming an RNA-induced silencing complex (RISC) that regulates gene expression. The RISC can modulate gene expression via perfect or imperfect base pairing to the 3'-untranslated region of the target mRNA, inducing target mRNA degradation or translational repression [41].

The binding of a miRNA occurs in its 5' "seed" region which is located at nucleotide bases 2-8. miRNAs usually bind imperfectly in animals, leading to translational repression [18]. In plants, miRNAs can bind perfectly leading to complete mRNA degradation [48]. While miRNAs do not often bind perfectly in animals, mRNA degradation can still occur following miRNA binding to the 3' UTR, resulting in recruitment of GW182 in *Drosophila* or TNRC6A–C docking protein in mammals. These proteins are needed for recruitment and attachment of a deadenylase protein complex. This complex consists of a group of deadenylases that interact with poly(A) binding proteins to dislodge adenines, and subsequently shorten the mRNA poly(A) tail. Additionally, the GW182 or TNRC6A–C protein recruits translational repressor proteins that interact with the 7-methyl-guanosine cap ( $m^7G$ ), destabilizing it leading to its removal [18]. The stable ends of the mRNA, 5'  $m^7G$  and 3' poly(A) tail, are removed and thus the mRNA is degraded [43].

Due to imperfect matching between the miRNA and its target in animals, one miRNA may regulate hundreds of mRNAs and as a result, may substantially affect gene networks [48]. miRNAs have been found to play important roles in early development, cellular differentiation, proliferation, apoptosis, and hematopoiesis [49-53]. They are also associated with immune response, insulin secretion, neurotransmitter syntheses, circadian

rhythm, and viral replication. It has been found that miRNAs influence cancers, neurodegenerative, heart, kidney, metabolic, immune, and liver diseases [41].

## **2.5. miRNA Skeletal Muscle Profiling in Type 2 Diabetes Mellitus**

The skeletal muscle miRNA profiling of normal glucose tolerant individuals, those with impaired glucose tolerance, and type 2 diabetics, revealed that there were significant alterations in miRNA expression. Out of 171 miRNAs expressed in skeletal muscle, 29 miRNAs were up-regulated and 33-downregulated in skeletal muscle from T2DM patients [54, 55]. Expression of miRNA differs when comparing rodent diabetic models to human investigations. The altered miRNA profile of rodent skeletal muscle correlates with 24 miRNAs in humans. However, it was found that the same miRNA displays differential expression in rodent skeletal muscle depending on the model used [16]. Differing methodology in analyzing the diabetic miRNA profile of rodent skeletal muscle causes difficulty in direct comparison. This suggests that the etiology of insulin resistance might influence the miRNA signature [16]. Also, the skeletal muscle type investigated differs between studies. For instance, the observation of soleus [55] and gastrocnemius [56], while other studies do not detail the specific skeletal muscle chosen to be profiled [57]. Overall, only few of the miRNAs identified to have differential expression in diabetic and insulin resistant models have been studied *in vitro* and *in vivo*.

## **2.6. miRNAs Affecting the Insulin Signaling Pathway**

Direct targeting of IRS-1 by miR-128a, miR-144 and let-7 has been found to influence the insulin signaling cascade [21, 58, 59]. miR-128a is a regulator of skeletal muscle myogenesis primarily through the targeting of IRS-1. It was shown that miR-128a

decreased myoblast proliferation determined by diminished cell count, and also decreased the protein expression of IRS-1, AKT, the insulin receptor (INSR), and PI3K in C2C12 cells [21]. When a miR-128a inhibitor was introduced *in vivo*, muscle hypertrophy was induced [21]. While it has been confirmed that miR-128a inhibits IRS-1, there are currently no studies elucidating its effects on signaling in insulin resistant states. miR-144 is highly upregulated in diabetic states, and was proven to target IRS-1 via an increase fold change in humans and rats with T2DM corresponding to a decrease in IRS-1 [56, 58]. The let-7 miRNA was shown to target insulin receptor substrate 2 (IRS-2), INSR, and insulin growth factor 1 receptor precursor. Through the use of a transgenic model, this study revealed that let-7 is repressed by lin28, and lin28 while being necessary for normal glucose metabolism and function is dependent on the mechanistic target of rapamycin (mTOR) [59].

In a high fat diet mouse model, miR-15b was upregulated and the INSR was shown to be a direct target [6, 60]. As miR-15b was overexpressed the expression of the INSR was decreased with and without the presence of insulin. This mechanism was shown to be controlled by palmitate, as palmitate caused increases in miR-15b and decreases in INSR over time [60]. This study observed these effects in hepatocytes and revealed that miR-15b expression was not influenced in skeletal muscle.

MiR-106b, miR-27a, miR-30d, miR-29a, miR-199a, miR-93, and miR-21 have all been found to play a role in insulin resistance through GLUT4 expression and activation [61-65]. In skeletal muscle of male Wister rats, overexpression of miR-106b, miR-27a, and miR-30d decreased glucose consumption, glucose uptake, expression of GLUT4, mitogen-activated protein kinase 14, and PI3K regulatory subunit beta. On the contrary,

silencing of these miRNAs enhanced each of these parameters, indicating the potential role of these miRNAs in the regulation of insulin resistance [61]. In C2C12 cells, miR-29a suppressed the expression of proliferator-activated receptor  $\delta$ , as well as altering the expression of GLUT4. When miR-29a was overexpressed, GLUT4 quantities were significantly decreased compared to controls [62].

Increased levels of miR-199a and miR-93 led to repression of GLUT4 expression, contributing to insulin resistance. Reduced glucose uptake via miR-199a can be rescued by GLUT4 overexpression, while miR-93 was found to directly target the 3' untranslated region of the GLUT4 gene in adipocytes [63, 64]. Contrary to the previous mentioned miRNAs, miR-21 overexpression increases phosphorylation of Akt, which enhances glucose translocation via GLUT4. This was found in insulin resistant 3T3-L1 adipocytes where miR-21 was found to be downregulated.

Recently, miR-194 expression was found to be downregulated by 25 – 50% *in vivo* in rats and humans with pre-diabetes and established diabetes [19]. However miR-194 inhibition in rat L6 myocytes resulted in increased basal and insulin stimulated glucose uptake, glycogen synthesis, glycolysis, Akt and glycogen synthase kinase 3 beta (GSK3 $\beta$ ) phosphorylation, and increase in mitochondrial oxidative phosphorylation [19]. Considering these conflicting results the authors concluded that early in T2DM development miR-194 acts as a stress-responsive miRNA and functions to increase muscle glucose uptake. Yet, while *in vitro* miR-194 inhibition increases glucose uptake, it is clearly not able to reverse insulin resistance *in vivo* displayed by the decreased expression in individuals with established T2DM [19]. The role miR-194 plays *in vivo* has not been observed.

## 2.7. The Effect of miR-26a on Insulin Signaling

A particular miRNA of interest to skeletal muscle insulin signaling is miR-26a. While large scale profiling of this miRNA has shown miR-26a expression to increase in gastrocnemius muscle in diabetic states [66] and during myogenesis [67], it has also been shown to decrease expression in liver with high fat diet feeding [22]. miR-26a directly targets the protein kinase isoforms responsible for impaired insulin signaling in hepatocytes. Interestingly, *In silico* mapping demonstrated high homology for the PKC $\theta$  isoform that impairs insulin signaling in skeletal muscle, further supporting a role for this miRNA in the regulation of insulin responsiveness. Furthermore, global or liver-specific overexpression of miR-26a through the use of transgenic mouse models improved parameters characteristic of type 2 diabetes mellitus [22]. Mice overexpressing miR-26a experienced improved insulin sensitivity, decreased hepatic glucose production, and decreased fatty acid synthesis, in hepatocytes challenged with a high fat diet [22]. This was achieved through the targeting of several key regulators of hepatic metabolism and insulin signaling.

Mainly, protein kinase C delta (PKC $\delta$ ) activity was decreased by miR-26a. PKC $\delta$  impairs IRS-1 activity, causing decreased phosphorylation of tyrosine residues activated when insulin binds to the IR. This reduces levels of phosphorylated AKT, altering glycogen synthesis and glucose uptake. Conversely, the silencing of endogenous miR-26a reversed these positive changes, revealing a role for miR-26a in regulated lipid induced hepatic insulin resistance. The role of miR-26a in skeletal muscle insulin signaling has yet to be explored. Yet, the evidence provided from the effect of miR-26a on liver tissue

and hepatocytes, coupled with the predicted complimentary base pairing of miR-26a to PKC $\theta$ , makes it a promising target for future studies.

## **2.8. Regulation of miR-26a**

Regulation of miR-26a is controlled through the activity of its host gene promotor, CTD small phosphatase-like protein (CTDSPL) [68]. CCAAT/enhancer-binding protein alpha (C/EBP $\alpha$ ) binds to the promotor region of CTDSPL increasing miR-26a which is located in the intron of the CTDSPL gene. C/EBP $\alpha$  is primarily regulated downstream through the activity of GSK3 $\beta$  [68]. When GSK3 $\beta$  is active it causes decreased glycogen synthesis and also decreased  $\beta$ -catenin expression. The decrease in  $\beta$ -catenin expression results in upregulation of C/EBP $\alpha$ , thus resulting in increased transcription of miR-26a in adipose-derived mesenchymal stem cells [68]. Figure 4 proposes how the regulation of miR-26a regulation may be important during lipid-induced skeletal muscle insulin resistance. Overexpression of miR-26a may inhibit the activity of kinases that interfere with insulin signaling, such as PTEN and PKC $\theta$ . A better understanding of how miR-26a fits in the paradigm of insulin signaling may unmask novel avenues for pharmacological and therapeutic interventions to help treat and/or prevent skeletal muscle lipid-induced insulin resistance.

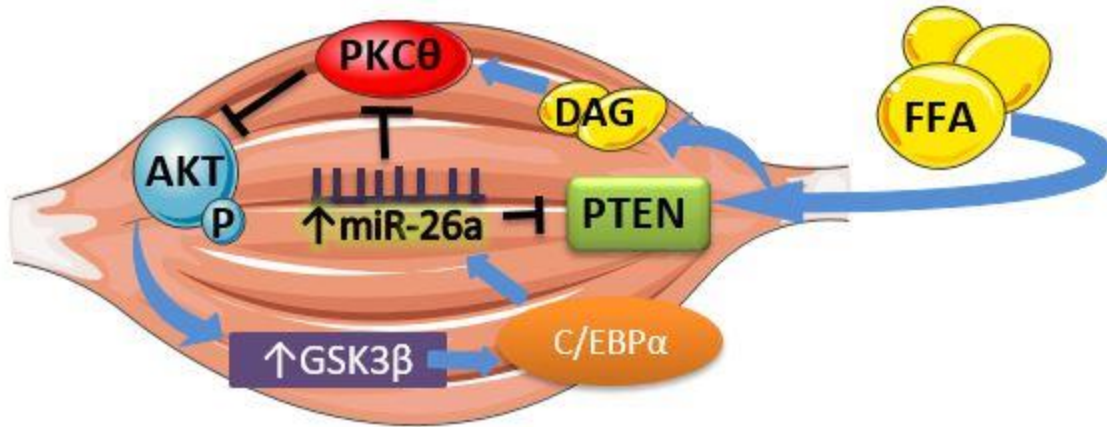


**Figure 4.** Proposed miR-26a regulation in skeletal muscle insulin signaling when challenged with free fatty acids (FFAs). Intracellular FFA accumulation increases diacylglycerol accumulation, activating PKCθ, a known inhibitor of insulin signaling. Additionally, FFAs increase PTEN expression, and protein levels. This results in reduced AKT phosphorylation and ultimately, increased miR-26a expression. Interestingly, PTEN and PKCθ are predicted targets of miR-26a. Therefore, it is plausible that miR-26a may regulate PTEN and PKCθ activity and serve as a target to enhance insulin responsiveness in skeletal muscle.

## 2.9. Conclusion

Ultimately, miRNAs may be useful tools to protect against the growing epidemic of T2DM. Current drugs and therapies for T2DM alleviate outcomes caused by the disease, but do not reverse or protect against the underlying root mechanisms. miRNAs are influential in the regulation of pathway communication in skeletal muscle and other types of cells [19, 21, 22, 58]. However, further research is needed in order to understand the role of miRNAs in skeletal muscle insulin signaling and their mechanism of regulation to accurately develop pharmacological interventions.

Additionally, the role of miRNAs in lipid induced myoblast insulin resistance is specifically interesting. Myoblast insulin responsiveness is a novel avenue to explore both mechanisms underlying dysregulated insulin signaling as well as muscle growth and regeneration. Both of these facets are integral to T2DM pathogenesis and assimilate to

contribute towards disease progression. The role that miR-26a plays in this process is promising towards unraveling the targets responsible for lipid induced insulin resistance. Thus, miR-26a may be an attractive therapeutic target and future research revealing the role of miR-26a in these processes is needed.

## CHAPTER 3: METHODS

### 3.1. Cell Culture and Treatment

Mouse C2C12 myoblasts were maintained at 37°C with 5% CO<sub>2</sub> in Dulbecco's modified eagle's medium (DMEM) containing 10% fetal bovine serum (FBS) and 1% penicillin/streptomycin. Immediately after seeding, cells were transfected with 100 µL of miRNA mimic complexes. Complexes consisted of 12% HiPerfect transfection reagent with miR-26a-5p mimic (Qiagen) at a concentration of 5 nM diluted in DMEM. When the C2C12 myoblasts reached ~90% confluence the cells were treated with 0.5 mM palmitic acid/10% FFA-Free BSA (FAF-BSA) diluted in 2% FAF-BSA/DMEM for 24 hours to induce insulin resistance *in vitro*. After palmitic acid incubation cells were treated with 100 nM insulin for 15 minutes prior to collection.

### 3.2. Palmitic Acid Solution

Palmitic acid (Cayman) was dissolved in 0.1 M NaOH while mixing and heating at 70°C to form a 150 mM solution. Palmitic acid was then diluted in 10% FAF-BSA/DMEM to 10 mM. FAF-BSA was diluted in DMEM to form a 10% FAF-BSA. 90% confluent myoblasts were treated with 0.5 mM palmitic acid/1% FAF-BSA/DMEM and with insulin as indicated above.

### 3.3. Experimental Design

C2C12 myoblasts comprised four separate groups (figure 5). (1) A control group that received NaOH and FAF-BSA/DMEM as a vehicle for palmitic acid, and 0.02 HCl with 1X phosphate buffered saline as a vehicle for insulin. In experiments involving miR-26a, the control group also received transfection reagent with a scramble sequence. (2)

An insulin group that received NaOH and FAF-BSA/DMEM as a vehicle for palmitic acid, and 100 nM insulin. In experiments involving miR-26a, the insulin group received transfection reagent with a scramble sequence. (3) A palmitic acid/insulin group that received 0.5 mM palmitic acid/1% FAF-BSA/DMEM and 100 nM insulin. In experiments involving miR-26a, the palmitic acid/insulin group received transfection reagent with a scramble sequence. (4) A miR-26a + palmitic acid/insulin group that received 0.5 mM palmitic acid/1% FAF-BSA/DMEM, and 100 nM insulin. This group also received transfection reagent and 5 nM miR-26a mimic. All groups were serum starved for 3 hour prior to treatment unless indicated.

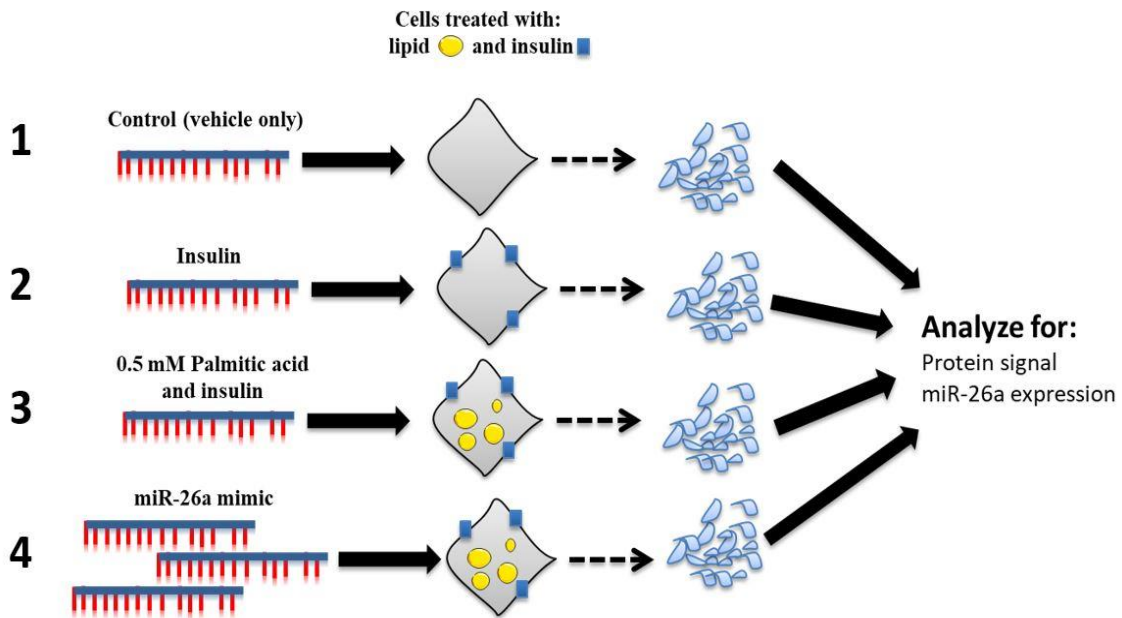


**Figure 5.** Experimental design used to assess how palmitic acid and insulin, and how miR-26a overexpression influences insulin responsiveness.

### **3.4. Western Blot Analysis**

Protein from cultured cells were extracted with RIPA buffer containing 1xprotease/phosphatase inhibitor cocktails. SDS-PAGE was performed using Nusep Tris-glycine precast gels. 15 µg of protein were loaded with 4x loading buffer. The proteins were separated at 150V for 60 minutes at 4°C. 0.45 µm pore size polyvinylidene fluoride membranes were activated using 100% methanol followed by a 2-min wash in deionized H<sub>2</sub>O. Electro blotting was carried out under 100V constant for 2 hours in Tris-glycine Transfer buffer supplemented with 10% methanol. Membranes were washed twice in Tris buffered saline (TBS) and blocked for 1 hour in Odyssey blocking buffer at room temperature. Blocking buffer was then removed and membranes washed twice in TBS-0.1% Tween (TBS-T). 16 hour incubation at 4°C with primary anti-bodies for phosphorylated AKT thr308 were diluted in 5% bovine serum albumin (BSA)-TBST at a concentration of 1:500. Total AKT, phosphorylated AKT ser473, PTEN, and β-actin were diluted in 5% BSA-TBST at a concentration of 1:1,000. Membranes were then washed twice in TBST and secondary antibodies diluted in 5% BSA-TBST at a concentration of 1:10,000 added for 2 hours at room temperature. Finally, two washes in TBST were followed by two washes in TBS before imaging on the Odyssey imaging system. Analysis of bands occurred using Odyssey software.

### **3.5. RNA Isolation and RT-qPCR**

Total RNA containing miRNAs were extracted from myoblasts using miRNeasy RNA isolation kit (Qiagen). Samples were reverse transcribed and converted into complementary DNA (cDNA) using the miScript II RT Kit (Qiagen) to assess miRNA and mRNA expression levels. Using miRNA specific primers (Qiagen) following the

























manufacturer's instructions, real time PCR was performed using the Step one Plus system (Applied Biosystems) using SYBR green from the miScript SYBR Green PCR Kit (Qiagen). Results were normalized to endogenous RNU6-2 and SNORD61, and fold change in expression levels was determined using  $2^{-\Delta\Delta CT}$ .

### **3.6. Bioinformatics Predictions**

To predict the target genes of miRNAs in the insulin signaling pathway, we utilized the scientifically certified miRNA target prediction databases: Targetscan ([www.targetscan.org](http://www.targetscan.org)) and miRanda ([www.microrna.org](http://www.microrna.org)).

### **3.7. miR-26a Dose Response**

A dose response experiment was completed for miRNA mimics. Figure 6 displays a format specified for transfection of C2C12 myoblasts in 24 well plates on the first day of cell seeding. Three concentrations of miRNA mimic were tested with three different concentrations of transfection reagent (TFR), and run against samples containing TFR only as controls. Cells were seeded at  $6 \times 10^4$  cells/cm<sup>2</sup> and incubated under normal growth conditions (37°C, 5% CO<sub>2</sub>). Concentrations of miRNA mimic at 1 nM, 5 nM, and 10 nM were tested with differing concentrations of transfection reagent to optimize the mimic: transfection reagent ratio. This was determined through a 24 hour incubation period with transfection complexes. Total RNA including miRNA was isolated as described above. This was followed by reverse transcription to form cDNA in order to view expression of miR-26a through RT-qPCR.

		1.5 $\mu$ l		3 $\mu$ l		4.5 $\mu$ l	
		1	2	3	4	5	6
Transfection Reagent only	<b>A</b>						
1nM (0.3 $\mu$ L)	<b>B</b>						
5nM (1.5 $\mu$ L)	<b>C</b>						
10nM (3 $\mu$ L)	<b>D</b>						

**Figure 6.** Optimization of miR-26a mimic and transfection reagent dose.

### 3.8. Flow Cytometry

C2C12 cells were plated in a 12-well plate at 48,000 cells per well and were transfected at seeding with DNA labeled to Alexa Fluor 488 (ThermoFisher) secondary antibody at different concentrations. Twenty-four hours post transfection, cells were treated with Cell Dissociation Buffer (Gibco) and analyzed using a BD Accuri C6 Flow Cytometer

### 3.9. Puromycin Decorporation

Myoblasts reached about 70% confluence and were then treated with 1  $\mu$ M puromycin for 24 hours. Cells were collected after 24 hours to serve as a positive control. Treatment groups were washed twice with 1X phosphate buffered saline, followed by PA treatment for 12 and 24 hours respectively. Anti-puromycin primary antibody was diluted

1:10,000 in 5% BSA-TBST for 16 hours. Secondary antibody was diluted 1:10,000 in 1X TBS.

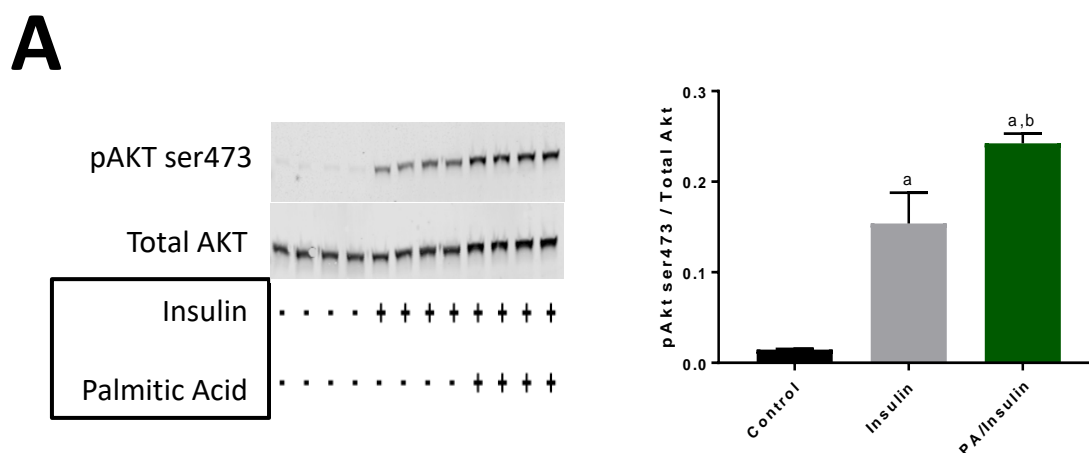
### **3.10. Statistical Analysis**

Statistical analyses was performed using Graph Pad Prism 7 software. To compare the effects of any treatment on more than two different groups of C2C12 myoblasts, we utilized a one-way analysis of variance (ANOVA). To analyze changes in endogenous miR-26a expression after PA treatment we ran an independent group t-test. To evaluate protein decorporation by treatment and time we utilized a two-way ANOVA. Tukey's post hoc was used to identify the source of significance with  $P < 0.05$ . The  $\alpha$  level was set at 0.05.

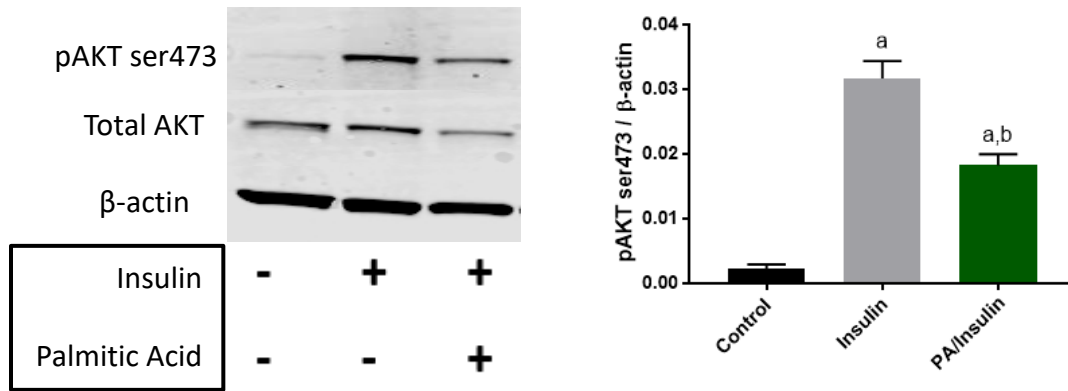
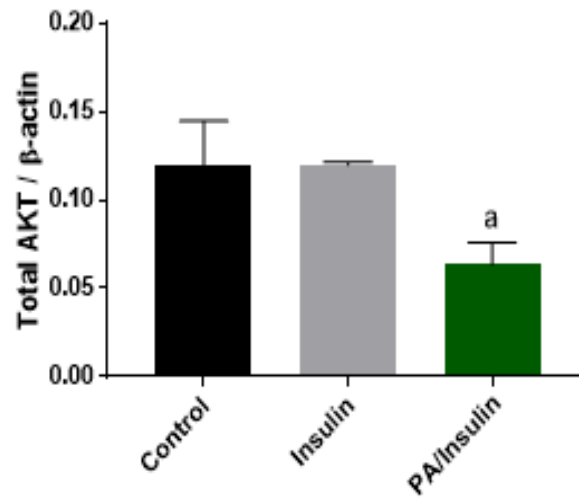
## CHAPTER 4: RESULTS

### 4.1. The Effect of PA Exposure on Insulin Responsiveness

To determine the effect of PA on insulin responsiveness, we exposed myoblast to PA for 2 (acute) or 24 hours of treatment (chronic). We then quantified changes in protein expression of AKT as a surrogate for insulin responsiveness. Phosphorylation of AKT at ser473 was significantly increased after 2 hours of PA and insulin treatment compared to insulin alone ( $P<0.001$ ) (figure 7A). However, AKT phosphorylation was significantly decreased after 24 hours of PA treatment normalized to  $\beta$ -actin ( $P<0.001$ ) (figure 7B). Due to PA treatment significantly decreasing total AKT after 24 hours of treatment, phosphorylation was compared to  $\beta$ -actin throughout (figure 7C). All cells were serum starved for 2 hours prior to treatment. Control groups received vehicles for all treatments, insulin groups received vehicles for all treatments and 100 nM insulin prior to collection, and the PA/insulin groups received 0.5 mM PA and 100 nM insulin.



**Figure 7.** The effect of palmitic acid exposure on insulin responsiveness. (A) C2C12 myoblasts (n=2) were treated in 0.5 mM PA for 2 hours in DMEM/1% pen-strep followed by 100 nM insulin for 20 minutes. This acute treatment resulted in a significant increase in phosphorylated AKT at serine residue 473 in the PA/insulin group vs. the insulin only group. Data was normalized to total AKT. Letter a signifies ( $P<0.0001$ ) compared to control, b signifies ( $P<0.001$ ) compared to insulin

**B****C**

**Figure 7, continued. (B)** Myoblasts (n=3) were also treated in 0.5 mM PA for 24 hours in 2% fatty acid free-BSA/DMEM followed by 100 nM insulin for 15 minutes. This chronic treatment resulted in a significant decrease in phosphorylated AKT at serine residue 473 in the PA/insulin group vs. the insulin only group. Data was normalized to β-actin. Letter a signifies ( $P<0.001$ ) compared to control, b signifies ( $P<0.001$ ) compared to insulin. **(C)** pAKTser473 was not normalized to total AKT in the 24 hour PA treatment as this chronic treatment resulted in a significant decrease in total AKT in the PA/insulin vs. the insulin only group. Letter a signifies ( $P<0.05$ ). All error bars represent SD.

#### 4.2. Palmitic Acid Treatment Decreases Endogenous Levels of miR-26a

Since 24 hour PA treatments reduced insulin signaling, we observed how this treatment influenced endogenous miR-26a expression. We found that exposure to PA for 24 hours, significantly reduced the expression of miR-26a in myoblasts compared to vehicle treated controls ( $P<0.05$ ) (figure 8). This indicates that miR-26a may regulate PA-induced insulin resistance in these cells.

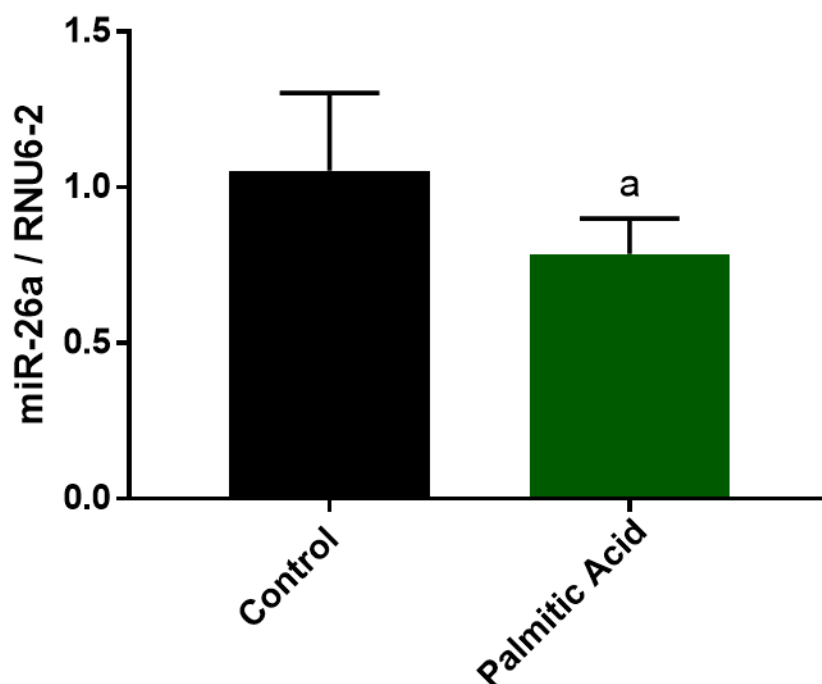


**Figure 8.** Palmitic acid treatment decreases endogenous levels of miR-26a. C2C12 myoblasts were treated with 0.5 mM PA diluted in DMEM/10% FBS/1% pen-strep for 24 hours (n=6). PA treatment significantly decreased endogenous miR-26a levels ( $P<0.05$ ), signified by the letter a. Error bars represent SD.

#### 4.3. Optimizing miR-26a Mimic in C2C12 Myoblasts

Since PA treatment reduced miR-26a expression, our next step was to overexpress miR-26a to determine if this would rescue PA-induced insulin resistance. To determine what concentration of miR-26a mimic should be used we conducted a dose response

experiment using real-time PCR and flow cytometry, respectively. The results showed that 5 nM miR-26a mimic significantly increased levels of miR-26a (figure 9A). Each group in figure 9A received HiPerfect Transfection Reagent and the indicated concentration of miR-26a, while the TFR group did not receive any miR-mimic. Next, transfection reagent efficiency was tested using flow cytometry. We observed a large increase in fluorescent signal in 5, 10, and 50 nM concentrations, indicating efficient transfection (figure 9B). In figure 9B all cells received different concentrations of fluorescently labeled DNA and HiPerfect Transfection Reagent, or no transfection reagent as indicated. In the histogram in figure 8B, the X-axis indicates fluorescence intensity and the Y-axis is the number of cells.

#### **4.4. miR-26a Overexpression Does Not Alter AKT Phosphorylation Following PA Exposure**

To assess how miR-26a influenced AKT phosphorylation in the presence of PA and insulin we overexpressed miR-26a and co-treated with PA and insulin. miR-26a overexpression did not significantly effect AKT ser 473 phosphorylation or total AKT normalized to  $\beta$ -actin in the presence of PA, compared to insulin only ( $P>0.05$ ) (figure 10). Additionally, miR-26a overexpression did not significantly effect AKT thr 308 phosphorylation. Lastly, miR-26a did not influence total AKT content that was decreased in both PA treated groups (figure 10).

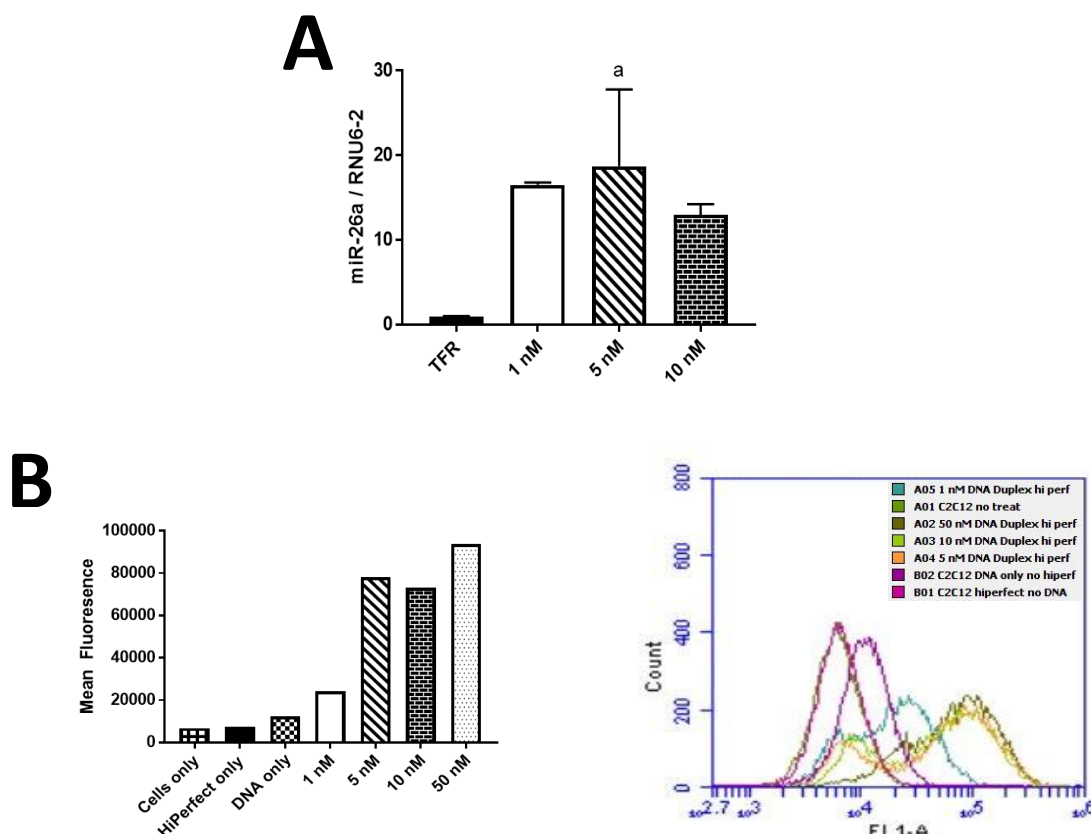


**Figure 9.** Optimization of miR-26a mimic. **(A)** C2C12 myoblasts (n=3) were treated with different concentrations of miR-26a mimic complexed to 7% transfection reagent (TFR). There was a significant difference between TFR only and the group that received 5 nM concentration ( $P < 0.05$ ), signified by letter a. **(B)** C2C12 myoblasts were transfected with different concentrations of fluorescently labeled DNA (Alexa Fluor 488) and 7% TFR. Mean fluorescence was determined by flow cytometry. Error bars represent SD.

#### 4.5. Palmitic Acid Decreases Endogenous Levels of PTEN in Myoblasts

PTEN is a target of miR-26a and a negative regulator of insulin signaling, thus we were interested in how levels of PTEN respond to PA treatment. To assess PTEN levels in myoblast insulin responsiveness we co-treated with PA, insulin, and miR-26a. PA treatment significantly decreased total PTEN in cells treated with PA/insulin and miR-26a mimic + PA/insulin, compared to insulin alone ( $P < 0.05$ , and  $P < 0.01$  respectively) (figure 11).

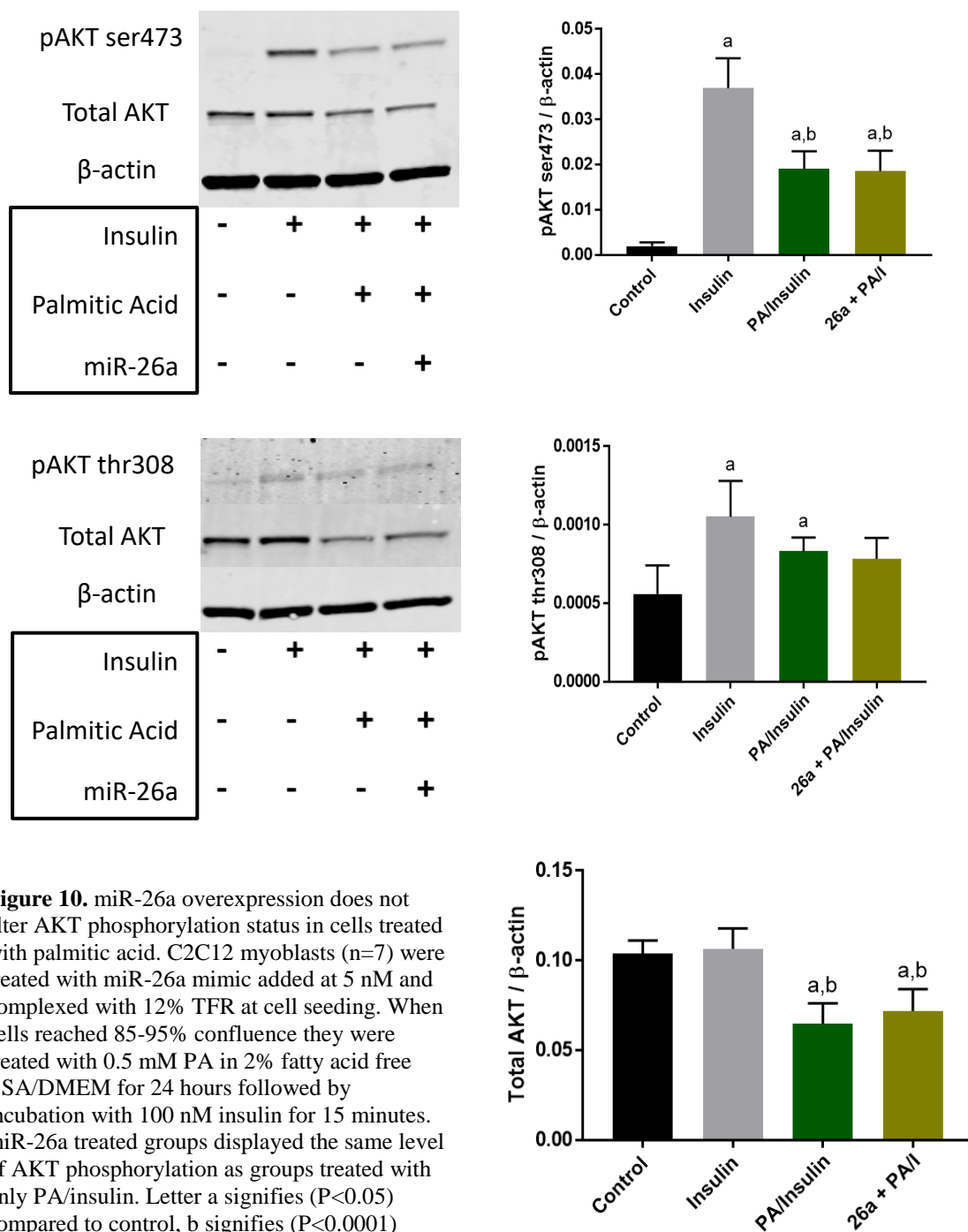


**Figure 10.** miR-26a overexpression does not alter AKT phosphorylation status in cells treated with palmitic acid. C2C12 myoblasts (n=7) were treated with miR-26a mimic added at 5 nM and complexed with 12% TFR at cell seeding. When cells reached 85-95% confluence they were treated with 0.5 mM PA in 2% fatty acid free BSA/DMEM for 24 hours followed by incubation with 100 nM insulin for 15 minutes. miR-26a treated groups displayed the same level of AKT phosphorylation as groups treated with only PA/insulin. Letter a signifies ( $P < 0.05$ ) compared to control, b signifies ( $P < 0.0001$ ) compared to insulin. All error bars represent SD.

#### 4.6. Palmitic Acid Does Not Increase Muscle Protein Breakdown in Myoblasts

Puromycin decorporation can be used as a measure of muscle protein breakdown. To identify if protein breakdown may have potentially caused PA associated decreases in protein, we utilized the puromycin decorporation approach. We observed that PA treatment did not significantly increase puromycin decorporation, and there was no significant interaction between treatment and time ( $F > 0.05$ ). However, there was a significant decrease in puromycin between 12 hour control and 24 hour control ( $P < 0.01$ ), 12 hour control and 24 hour PA ( $P < 0.01$ ), and 12 hour PA and 24 hour PA ( $P < 0.05$ ) (figure 12). This designates that time influenced muscle protein breakdown but PA treatment did not.

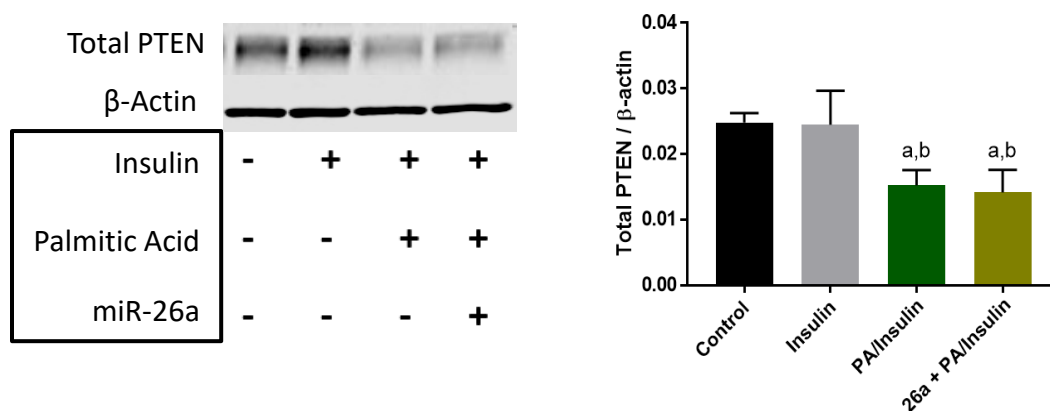


**Figure 11.** Palmitic acid decreases endogenous levels of PTEN. C2C12 myoblasts ( $n=4$ ) were treated with miR-26a mimic added at 5 nM and complexed with 12% TFR at cell seeding. When cells reached 85-95% confluence they were treated with 0.5 mM PA in 2% fatty acid free BSA/DMEM for 24 hours followed by incubation with 100 nM insulin for 15 minutes. PA treatment significantly decreased levels of PTEN in the PA/insulin group and the miR-26a + PA/insulin group, letter a signifies ( $P < 0.01$ ) compared to control, b signifies ( $P < 0.05$ ) compared to insulin. All error bars represent SD.

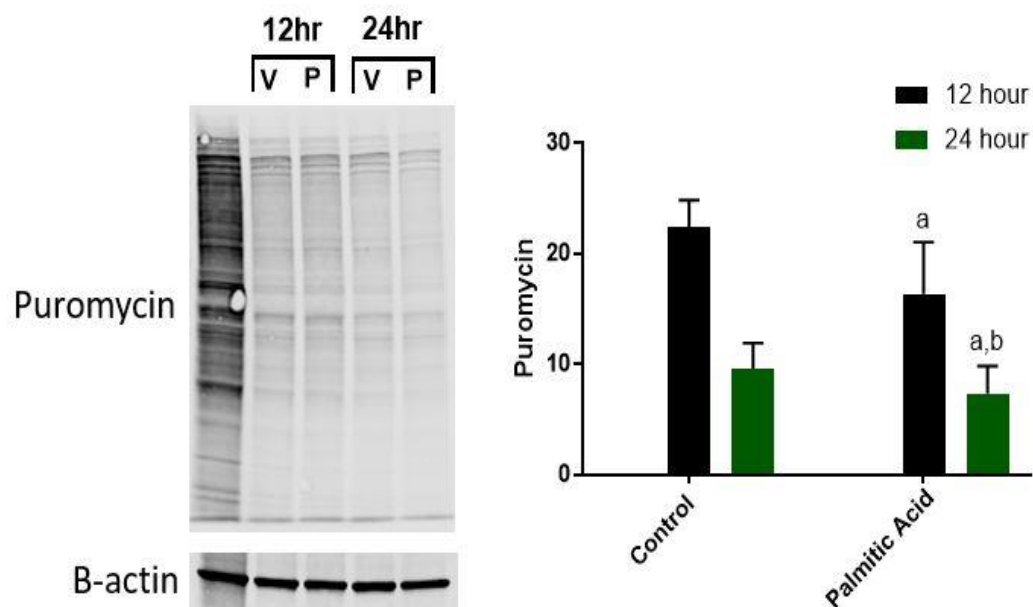


**Figure 12.** Muscle protein breakdown measured by puromycin incorporation. C2C12 myoblasts (n=3) were treated with 1  $\mu$ M puromycin for 24 hours. Cells were then treated with 0.5 mM PA for 12 or 24 hours then collected. Letter a signifies ( $P<0.01$ ) compared to 12 hour control, b signifies ( $P<0.05$ ) compared to 12 hour PA. Error bars represent SD.

## CHAPTER 5: DISCUSSION

Intramyocellular lipid accumulation is commonly found in individuals with T2DM [5]. The increase in ectopic lipid accumulation in skeletal muscle disrupts metabolism and results in skeletal muscle insulin resistance [6, 13]. Additionally, impaired insulin signaling in muscle reduces muscle growth and regenerative capacity, further limiting skeletal muscles ability to dispose of glucose. Investigating how miRNAs influence insulin resistance pathogenesis may provide promising pharmacological interventions. However, understanding the role that miRNAs have in skeletal muscle metabolism and insulin signaling is still in its infancy. Most of the research focuses on miRNA expression changes in muscle of different diabetic animal models, or human tissue of individuals with T2DM or glucose intolerance [16]. It is known that some miRNAs have functional roles in disease progression such as miR-106b, which decreases mitochondrial fusion leading to increased oxidative stress and ultimately decreased glucose uptake [20].

Our study examined how miR-26a influences myoblast insulin responsiveness in the presence of PA, a known inducer of insulin resistance. In our study, we show that not only does phosphorylated AKT decreased with PA treatment, but total AKT protein is also attenuated. For insulin mediated myogenesis to occur AKT signaling is required [38]. The reduction in myoblast AKT with PA treatment indicates saturated fatty acids reduce the cells ability to continue through the myogenic program. However, PA treatment decreased PTEN protein indicative of an enhanced proliferative state [69]. Research investigating how PA influences myoblasts exhibits that PA decreases their proliferative capacity [70]. The mechanism was partly attributed to a decrease in cell

cycle progression proteins cyclin A and cyclin D1, and an increase in cell cycle inhibitory protein p21-cdk4 complex formation with PA treatment [70]. It is plausible that the PA treatment reduces proliferative capacity, and when introducing insulin that promotes myogenesis the cell attempts to begin the myogenic program. Yet, the AKT needed for insulin action is reduced by PA thus eliminating the positive effects insulin has on myogenesis.

In addition to inhibited myoblast proliferative capacity it has also been shown that PA decreases many gene networks within the cell. The biological pathways most affected by PA involved signal transduction genes, which encompasses the genes analyzed in our study [71]. Included in this gene dysregulation, are 11 genes in the PI3K cascade and 8 genes in the insulin signaling/AKT pathway [71]. This could explain the lack of effect overexpressing miR-26a had on insulin signaling. We show that there is a decrease in total AKT, and PTEN proteins after PA treatment in myoblasts. If the decrease in protein is due to negative gene regulation this would result in reduced mRNA transcript content. miRNAs need to interact with the 3'UTR of mRNA transcripts to induce a repression effect. Thus, the reduction in total gene output would render the miRNA useless, as it is a post transcriptional regulator (figure 13). Additionally, we show that protein degradation observed through puromycin incorporation was not the cause of decreased total protein content. Yet, it is conceivable that PA interferes with miRNA transfection or the biogenesis/transport machinery as this was not explored in our study.

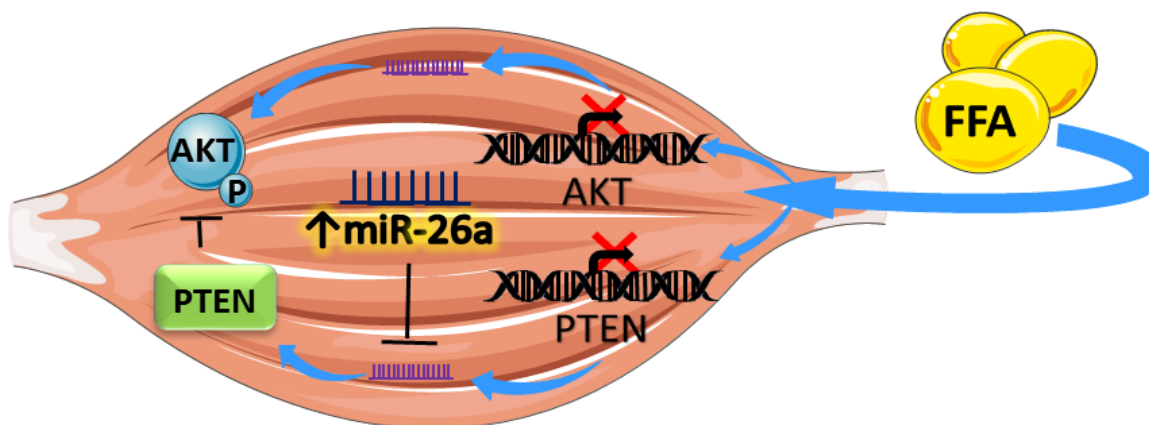


**Figure 13.** Proposed mechanism of palmitic acid effects on skeletal muscle cells. In our study, we observed decreased levels of total AKT and PTEN in groups given PA. The results may be indicative of decreased gene transcription of AKT and PTEN, as it has been observed that PA causes decreased expression of genes in the insulin/AKT and PI3K signaling cascades in myoblasts. Thus, this indicates that metabolic deficiency caused by PA may be a gene regulatory mechanism opposed to impaired intracellular signaling.

Interestingly, we also observed an increase in insulin sensitivity with acute PA treatment. Pu et al, also observed an increase in AKT phosphorylation with acute PA treatment [72]. It was observed that palmitate needed to interact with proteins at the plasma membrane in order to induce this enhanced phosphorylation effect. Post prandial fatty acid levels fluctuate and this mechanism of increasing insulin signaling may be a means of regulating circulating fatty acid levels [72]. If fatty acids levels remain elevated the negative effects of chronic exposure begin to develop.

Ultimately, the results of our study contribute to the knowledge of skeletal muscle tissue maintenance. The ectopic lipid build up seen in muscle tissue of T2DM patients causes insulin resistance, causing hyperglycemia. Though, this dysregulated lipid accumulation also inhibits skeletal muscle injury repair and regrowth, which is essential towards preserving muscle health. These impairments amass as reduction in healthy muscle further impairs glucose uptake capacity as well as decreases the ability to utilize

exercise as an intervention to combat T2DM pathogenesis. Understanding the mechanisms of how insulin resistance ensues may contribute to development of therapeutics that alleviate both issues. We looked to investigate the role of miR-26a in myoblast insulin responsiveness to potentially address a novel molecule useful as a pharmacological target. We elucidated that the lipid induced mechanism of myoblast insulin resistance is not reversible by increasing miR-26a in our model. However, we did discover that PA treatment in combination with insulin may alter the myogenic program through reductions in AKT. Additionally, we provide a potential mechanism explaining how myoblast insulin resistance occurs, and why miRNAs may not be viable in the myoblast-PA treated environment.

## CHAPTER 6: CONCLUSION

In conclusion, our study revealed that PA disrupts insulin responsiveness in C2C12 myoblasts. We observed the role of miR-26a in skeletal muscle cell insulin response when challenged with PA. The results of our study indicate that miR-26a may not have a central role in preserving insulin responsiveness when myoblasts are treated with PA. However, we did disclose that PA causes reductions in AKT protein in myoblasts. The effects of PA on myoblasts suggests that saturated fatty acids may negatively impact skeletal muscle growth and regeneration, providing implications for developmental and injury induced muscle defects in T2DM pathogenesis. The precise mechanisms of how PA causes these changes in myoblasts may be a topic of future research.

## REFERENCES

1. Collaboration, N.C.D.R.F., *Worldwide trends in diabetes since 1980: a pooled analysis of 751 population-based studies with 4.4 million participants*. Lancet, 2016. **387**(10027): p. 1513-30.
2. DeFronzo, R.A., *Pathogenesis of type 2 diabetes mellitus*. Med Clin North Am, 2004. **88**(4): p. 787-835, ix.
3. Li, Y., et al., *Skeletal intramyocellular lipid metabolism and insulin resistance*. Biophys Rep, 2015. **1**: p. 90-98.
4. Kuhlmann, J., et al., *Intramyocellular lipid and insulin resistance: a longitudinal in vivo <sup>1</sup>H-spectroscopic study in Zucker diabetic fatty rats*. Diabetes, 2003. **52**(1): p. 138-44.
5. Hegarty, B.D., et al., *The role of intramuscular lipid in insulin resistance*. Acta Physiol Scand, 2003. **178**(4): p. 373-83.
6. Samuel, V.T. and G.I. Shulman, *Mechanisms for insulin resistance: common threads and missing links*. Cell, 2012. **148**(5): p. 852-71.
7. Peck, B., et al., *Mice lacking PKC- $\theta$  in skeletal muscle have reduced intramyocellular lipid accumulation and increased insulin responsiveness in skeletal muscle*. Am J Physiol Regul Integr Comp Physiol, 2018. **314**(3): p. R468-R477.
8. Kalyani, R.R., M. Corriere, and L. Ferrucci, *Age-related and disease-related muscle loss: the effect of diabetes, obesity, and other diseases*. Lancet Diabetes Endocrinol, 2014. **2**(10): p. 819-29.
9. DeFronzo, R.A. and D. Tripathy, *Skeletal muscle insulin resistance is the primary defect in type 2 diabetes*. Diabetes Care, 2009. **32 Suppl 2**: p. S157-63.
10. Savage, D.B., K.F. Petersen, and G.I. Shulman, *Disordered lipid metabolism and the pathogenesis of insulin resistance*. Physiol Rev, 2007. **87**(2): p. 507-20.
11. Li, Y., et al., *Protein kinase C  $\theta$  inhibits insulin signaling by phosphorylating IRS1 at Ser(1101)*. J Biol Chem, 2004. **279**(44): p. 45304-7.
12. Hu, Z., et al., *PTEN expression contributes to the regulation of muscle protein degradation in diabetes*. Diabetes, 2007. **56**(10): p. 2449-56.
13. Samuel, V.T. and G.I. Shulman, *The pathogenesis of insulin resistance: integrating signaling pathways and substrate flux*. J Clin Invest, 2016. **126**(1): p. 12-22.

14. Yaffe, D. and O. Saxel, *Serial passaging and differentiation of myogenic cells isolated from dystrophic mouse muscle*. Nature, 1977. **270**(5639): p. 725-7.
15. Chal, J. and O. Pourquie, *Making muscle: skeletal myogenesis in vivo and in vitro*. Development, 2017. **144**(12): p. 2104-2122.
16. Massart, J., M. Katayama, and A. Krook, *microManaging glucose and lipid metabolism in skeletal muscle: Role of microRNAs*. Biochim Biophys Acta, 2016.
17. Bartel, D.P., *MicroRNAs: genomics, biogenesis, mechanism, and function*. Cell, 2004. **116**(2): p. 281-97.
18. Iwakawa, H.O. and Y. Tomari, *The Functions of MicroRNAs: mRNA Decay and Translational Repression*. Trends Cell Biol, 2015. **25**(11): p. 651-65.
19. Latouche, C., et al., *MicroRNA-194 Modulates Glucose Metabolism and Its Skeletal Muscle Expression Is Reduced in Diabetes*. PLoS One, 2016. **11**(5): p. e0155108.
20. Zhang, Y., et al., *Silencing miR-106b improves palmitic acid-induced mitochondrial dysfunction and insulin resistance in skeletal myocytes*. Mol Med Rep, 2015. **11**(5): p. 3834-41.
21. Motohashi, N., et al., *Regulation of IRS1/Akt insulin signaling by microRNA-128a during myogenesis*. J Cell Sci, 2013. **126**(Pt 12): p. 2678-91.
22. Fu, X., et al., *MicroRNA-26a regulates insulin sensitivity and metabolism of glucose and lipids*. J Clin Invest, 2015. **125**(6): p. 2497-509.
23. Whitehead, J.P., et al., *Signaling through the insulin receptor*. Curr Opin Cell Biol, 2000. **12**(2): p. 222-8.
24. Saltiel, A.R. and C.R. Kahn, *Insulin signalling and the regulation of glucose and lipid metabolism*. Nature, 2001. **414**(6865): p. 799-806.
25. Karp, G., *Cell and molecular biology : concepts and experiments*. 7th ed. 2013, Hoboken, NJ: John Wiley. xvi, 783 pages.
26. Boucher, J., A. Kleinridders, and C.R. Kahn, *Insulin receptor signaling in normal and insulin-resistant states*. Cold Spring Harb Perspect Biol, 2014. **6**(1).
27. Szendroedi, J., et al., *Role of diacylglycerol activation of PKC $\theta$  in lipid-induced muscle insulin resistance in humans*. Proc Natl Acad Sci U S A, 2014. **111**(26): p. 9597-602.

28. Lima, M.H., et al., *Regulation of IRS-1/SHP2 interaction and AKT phosphorylation in animal models of insulin resistance*. Endocrine, 2002. **18**(1): p. 1-12.
29. Sun, X.J., et al., *Expression and function of IRS-1 in insulin signal transmission*. J Biol Chem, 1992. **267**(31): p. 22662-72.
30. Virkamaki, A., K. Ueki, and C.R. Kahn, *Protein-protein interaction in insulin signaling and the molecular mechanisms of insulin resistance*. J Clin Invest, 1999. **103**(7): p. 931-43.
31. Lo, Y.T., et al., *Increase of PTEN gene expression in insulin resistance*. Horm Metab Res, 2004. **36**(10): p. 662-6.
32. Wijesekara, N., et al., *Muscle-specific Pten deletion protects against insulin resistance and diabetes*. Mol Cell Biol, 2005. **25**(3): p. 1135-45.
33. Teresi, R.E., et al., *Increased PTEN expression due to transcriptional activation of PPARgamma by Lovastatin and Rosiglitazone*. Int J Cancer, 2006. **118**(10): p. 2390-8.
34. Maruyama, H., et al., *Palmitate-induced Regulation of PPARgamma via PGC1alpha: a Mechanism for Lipid Accumulation in the Liver in Nonalcoholic Fatty Liver Disease*. Int J Med Sci, 2016. **13**(3): p. 169-78.
35. Shepherd, P.R. and B.B. Kahn, *Glucose transporters and insulin action--implications for insulin resistance and diabetes mellitus*. N Engl J Med, 1999. **341**(4): p. 248-57.
36. Burattini, S., et al., *C2C12 murine myoblasts as a model of skeletal muscle development: morpho-functional characterization*. Eur J Histochem, 2004. **48**(3): p. 223-33.
37. Conejo, R. and M. Lorenzo, *Insulin signaling leading to proliferation, survival, and membrane ruffling in C2C12 myoblasts*. J Cell Physiol, 2001. **187**(1): p. 96-108.
38. Conejo, R., et al., *Insulin produces myogenesis in C2C12 myoblasts by induction of NF-kappaB and downregulation of AP-1 activities*. J Cell Physiol, 2001. **186**(1): p. 82-94.
39. Collins, K.H., et al., *Obesity, Metabolic Syndrome, and Musculoskeletal Disease: Common Inflammatory Pathways Suggest a Central Role for Loss of Muscle Integrity*. Front Physiol, 2018. **9**: p. 112.

40. Karalaki, M., et al., *Muscle regeneration: cellular and molecular events*. In Vivo, 2009. **23**(5): p. 779-96.
41. Zhang, X., et al., *MicroRNA Detection and Pathological Functions*, in *SpringerBriefs in Molecular Science*,. 2015. p. IX, 101 p. 47 illus., 45 illus. in color.
42. Lee, R.C., R.L. Feinbaum, and V. Ambros, *The C. elegans heterochronic gene lin-4 encodes small RNAs with antisense complementarity to lin-14*. Cell, 1993. **75**(5): p. 843-54.
43. Bartel, D.P., *MicroRNAs: target recognition and regulatory functions*. Cell, 2009. **136**(2): p. 215-33.
44. Ambros, V., *The functions of animal microRNAs*. Nature, 2004. **431**(7006): p. 350-5.
45. Pillai, R.S., *MicroRNA function: multiple mechanisms for a tiny RNA?* RNA, 2005. **11**(12): p. 1753-61.
46. Rossi, J.J. and G.J. Hannon, *MicroRNA methods*, in *Methods in enzymology*,. 2007, Academic Press,: San Diego, Calif. p. 1 online resource (xl, 261 p., 8 p. of plates).
47. Asgari, S., *Role of MicroRNAs in Insect Host-Microorganism Interactions*. Front Physiol, 2011. **2**: p. 48.
48. Ambros, V., *microRNAs: tiny regulators with great potential*. Cell, 2001. **107**(7): p. 823-6.
49. Park, H., et al., *MicroRNA-146a and microRNA-146b regulate human dendritic cell apoptosis and cytokine production by targeting TRAF6 and IRAK1 proteins*. J Biol Chem, 2015. **290**(5): p. 2831-41.
50. Liu, Y., et al., *MicroRNA-124 Targets Tip110 Expression and Regulates Hematopoiesis*. Stem Cells Dev, 2015. **24**(17): p. 2009-17.
51. Kim, H.K., et al., *Muscle-specific microRNA miR-206 promotes muscle differentiation*. J Cell Biol, 2006. **174**(5): p. 677-87.
52. Chen, J.F., et al., *The role of microRNA-1 and microRNA-133 in skeletal muscle proliferation and differentiation*. Nat Genet, 2006. **38**(2): p. 228-33.
53. Song, J.L., et al., *Select microRNAs are essential for early development in the sea urchin*. Dev Biol, 2012. **362**(1): p. 104-13.

54. Gallagher, I.J., et al., *Integration of microRNA changes in vivo identifies novel molecular features of muscle insulin resistance in type 2 diabetes*. Genome Med, 2010. **2**(2): p. 9.
55. Herrera, B.M., et al., *Global microRNA expression profiles in insulin target tissues in a spontaneous rat model of type 2 diabetes*. Diabetologia, 2010. **53**(6): p. 1099-109.
56. Chen, G.Q., et al., *Altered microRNA expression in skeletal muscle results from high-fat diet-induced insulin resistance in mice*. Mol Med Rep, 2012. **5**(5): p. 1362-8.
57. Huang, B., et al., *MicroRNA expression profiling in diabetic GK rat model*. Acta Biochim Biophys Sin (Shanghai), 2009. **41**(6): p. 472-7.
58. Karolina, D.S., et al., *MicroRNA 144 impairs insulin signaling by inhibiting the expression of insulin receptor substrate 1 in type 2 diabetes mellitus*. PLoS One, 2011. **6**(8): p. e22839.
59. Zhu, H., et al., *The Lin28/let-7 axis regulates glucose metabolism*. Cell, 2011. **147**(1): p. 81-94.
60. Yang, W.M., et al., *Obesity-induced miR-15b is linked causally to the development of insulin resistance through the repression of the insulin receptor in hepatocytes*. Mol Nutr Food Res, 2015. **59**(11): p. 2303-14.
61. Zhou, T., et al., *Regulation of Insulin Resistance by Multiple MiRNAs via Targeting the GLUT4 Signalling Pathway*. Cell Physiol Biochem, 2016. **38**(5): p. 2063-78.
62. Zhou, Y., et al., *MicroRNA-29a induces insulin resistance by targeting PPARdelta in skeletal muscle cells*. Int J Mol Med, 2016. **37**(4): p. 931-8.
63. Yan, S.T., et al., *MiR-199a is overexpressed in plasma of type 2 diabetes patients which contributes to type 2 diabetes by targeting GLUT4*. Mol Cell Biochem, 2014. **397**(1-2): p. 45-51.
64. Chen, Y.H., et al., *miRNA-93 inhibits GLUT4 and is overexpressed in adipose tissue of polycystic ovary syndrome patients and women with insulin resistance*. Diabetes, 2013. **62**(7): p. 2278-86.
65. Ling, H.Y., et al., *MiRNA-21 reverses high glucose and high insulin induced insulin resistance in 3T3-L1 adipocytes through targeting phosphatase and tensin homologue*. Exp Clin Endocrinol Diabetes, 2012. **120**(9): p. 553-9.

66. Mohamed, J.S., et al., *MicroRNA-149 inhibits PARP-2 and promotes mitochondrial biogenesis via SIRT-1/PGC-1alpha network in skeletal muscle*. Diabetes, 2014. **63**(5): p. 1546-59.
67. Dey, B.K., et al., *miR-26a is required for skeletal muscle differentiation and regeneration in mice*. Genes Dev, 2012. **26**(19): p. 2180-91.
68. Wang, Z., et al., *A regulatory loop containing miR-26a, GSK3beta and C/EBPalpha regulates the osteogenesis of human adipose-derived mesenchymal stem cells*. Sci Rep, 2015. **5**: p. 15280.
69. Yue, F., et al., *Conditional Loss of Pten in Myogenic Progenitors Leads to Postnatal Skeletal Muscle Hypertrophy but Age-Dependent Exhaustion of Satellite Cells*. Cell Rep, 2016. **17**(9): p. 2340-2353.
70. Grabiec, K., et al., *Palmitate exerts opposite effects on proliferation and differentiation of skeletal myoblasts*. Cell Biol Int, 2015. **39**(9): p. 1044-52.
71. Grabiec, K., et al., *The effect of palmitate supplementation on gene expression profile in proliferating myoblasts*. Cell Biol Toxicol, 2016. **32**(3): p. 185-98.
72. Pu, J., et al., *Palmitic acid acutely stimulates glucose uptake via activation of Akt and ERK1/2 in skeletal muscle cells*. J Lipid Res, 2011. **52**(7): p. 1319-27.

## APPENDIX: ORIGINAL WESTERN BLOTS USED FOR ANALYSIS

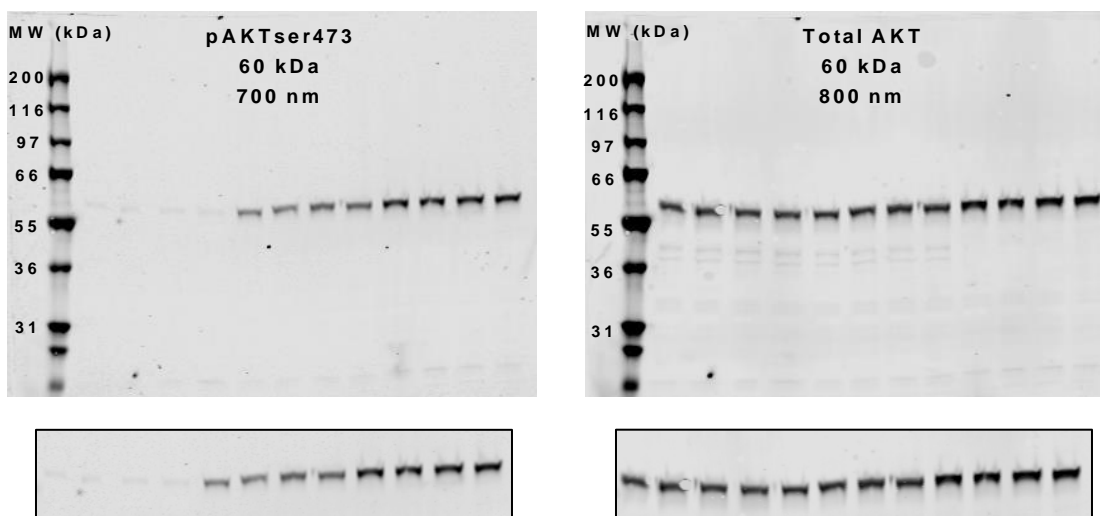


Image from which figure 7A was derived. Shown above to the left is expression of phosphorylated AKT serine 473 at the molecular weight of 60 kilodaltons (kDa). This is displayed from 700 nm wavelength. Shown above to the right is expression of total AKT at the molecular weight of 60 kDa. This is displayed from the 800 nm wavelength. Below each image is what is represented in figure 7A.

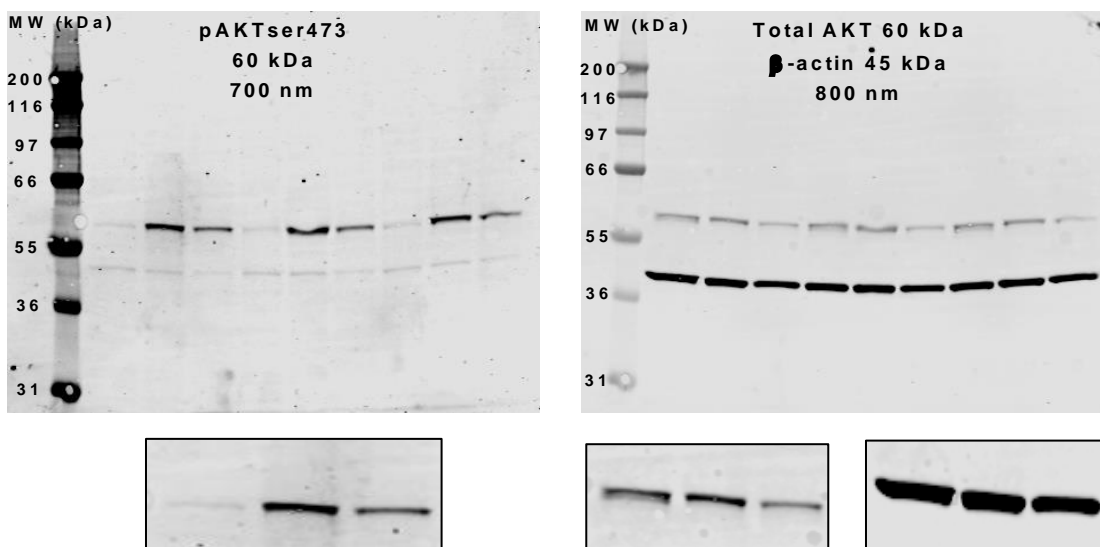


Image from which figure 7B was derived. Shown above to the left is expression of phosphorylated AKT serine 473 at the molecular weight of 60 kDa. This is displayed from the 700 nm wavelength. Shown above to the right is expression of total AKT at the molecular weight of 60 kDa and  $\beta$ -actin at the molecular weight of 45 kDa. This is

displayed from the 800 nm wavelength. Below each image is what is represented in figure 7B, and was cropped from the first three bands of each blot.

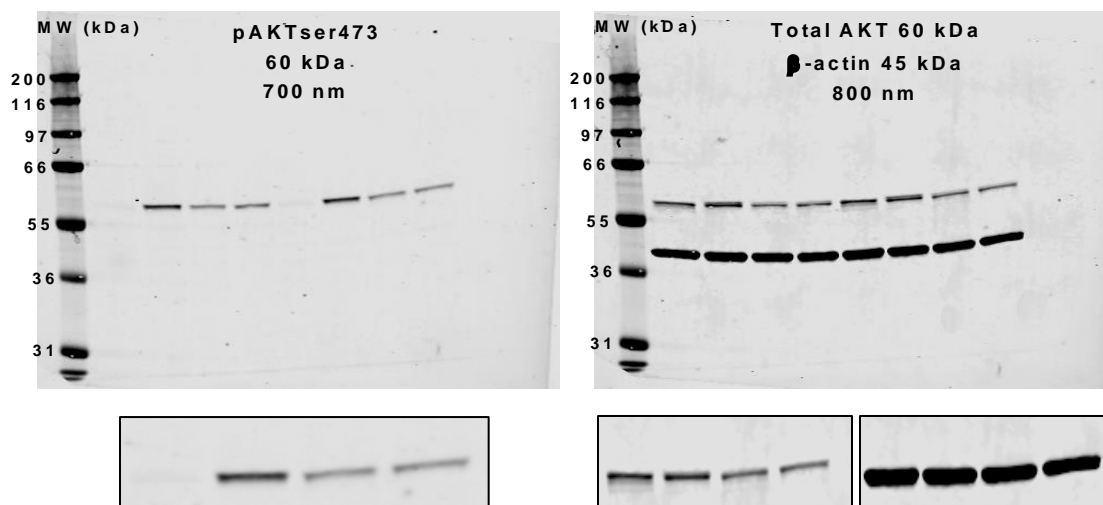


Image from which figure 10 was derived. Shown above to the left is expression of phosphorylated AKT serine 473 at the molecular weight of 60 kDa. This is displayed from the 700 nm wavelength. Shown above to the right is expression of total AKT at the molecular weight of 60 kDa, and β-actin at the molecular weight of 45 kDa. This is displayed from the 800 nm wavelength. Below each image is what is represented in figure 10, and was cropped from the last four bands of each blot.

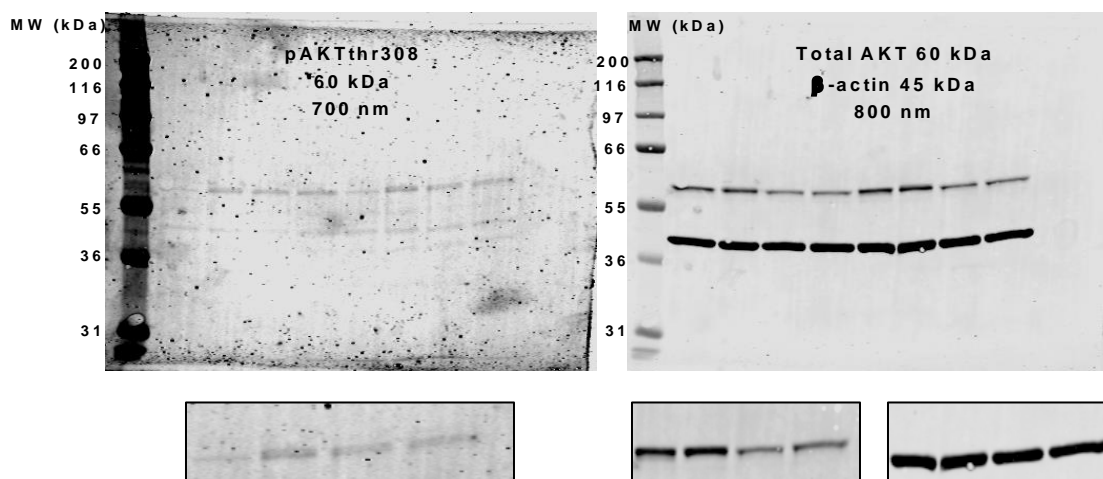


Image above from which figure 10 was derived. Shown above to the left is expression of phosphorylated AKT threonine 308 at the molecular weight of 60 kDa. This is displayed from the 700 nm wavelength. Shown above to the right is expression of total AKT at the

molecular weight of 60 kDa and  $\beta$ -actin at the molecular weight of 45 kDa. This is displayed from the 800 nm wavelength. Below each image is what is represented in figure 10, and was cropped from last four bands.

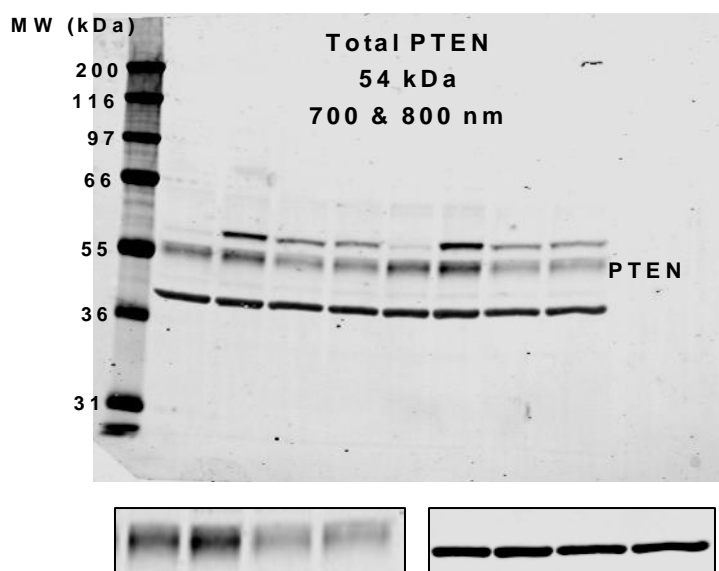


Image from which figure 11 was derived. Shown above is expression of phosphorylated AKT serine 473 at the molecular weight of 60 kDa, total PTEN at the molecular weight of 54 kDa, and  $\beta$ -actin at the molecular weight of 45 kDa. This image is displaying both 700 and 800 nm wavelengths. Only total PTEN and  $\beta$ -actin were displayed in figure 11. Below each image is what is represented in figure 11, and was cropped from the last four bands.

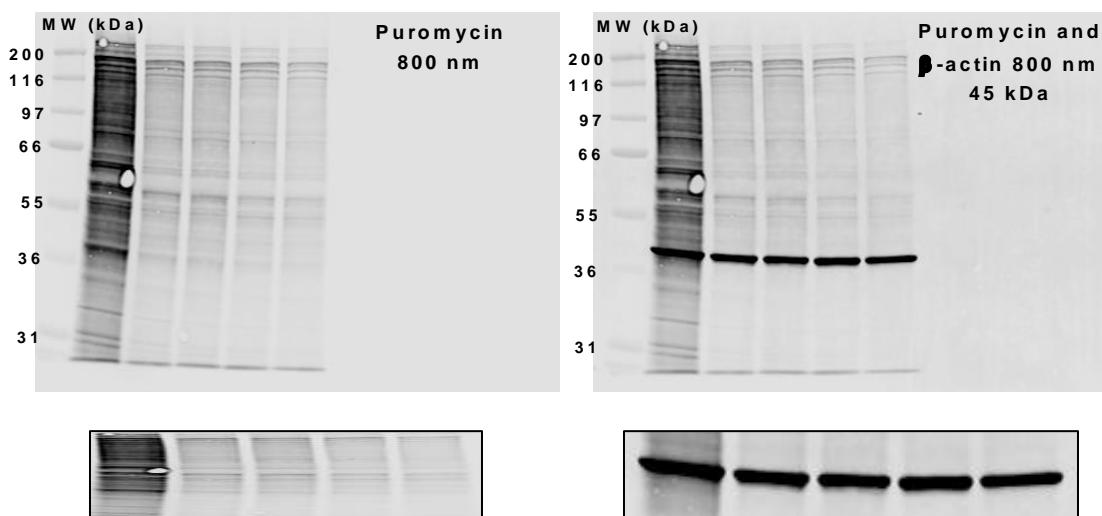


Image from which figure 12 was derived. Shown above to the left is expression of puromycin which stains all newly synthesized proteins. Thus, expression is shown spanning all molecular weights separated by this gel. This image is displayed in the 800 nm wavelength. Shown above to the right is expression of puromycin as well as  $\beta$ -actin at the molecular weight of 45 kDa. This is displayed from the 800 nm wavelength. Below each image is what is represented in figure 12.